ANALYSIS OF UNFROZEN WATER IN CATION-TREATED, FINE-GRAINED SOILS USING THE PULSE NUCLEAR MAGNETIC RESONANCE (P-NMR) METHOD

By

Aaron M. Kruse, B.S.

A Thesis Submitted in Partial Fulfillment of the Requirements

for the Degree of

Masters of Science

in

Geological Engineering

University of Alaska Fairbanks

December 2016

APPROVED:

Dr. Margaret M. Darrow, Committee Chair
Dr. Paul A. Metz, Committee Member
Dr. Thomas P. Trainor, Committee Member
Dr. Margaret M. Darrow, Chair
Department of Mining and Geological Engineering
Dr. Douglas J. Goering, Dean
College of Engineering and Mines
Dr. Michael A. Castellini
Dean of the Graduate School

Abstract

Unfrozen water within frozen soils is a key component that determines a soil's thermophysical response to changing physical and environmental conditions. This research focuses on the use of pulse nuclear magnetic resonance (P-NMR) for measuring unfrozen water content within frozen soils. The research is divided into two components: 1) improvements made to the P-NMR testing method, including refinements in the laboratory set up and testing procedure, and experimental validation of the normalization method; and 2) determination of unfrozen water content of fine-grained, cation-treated samples at various sub-freezing temperatures using the improved P-NMR methodology. Previous P-NMR testing used the first return data from the free induction decay signal intensity to calculate unfrozen water content; however, this approach may overestimate unfrozen water due to inclusion of ice content. This research used the normalization method for calculating unfrozen water, which proved to be repeatable with excellent agreement between P-NMR-derived unfrozen water and physical gravimetric water content data. Cation treatments of five standard clays and one heterogeneous soil were prepared to determine how the physicochemical structure of clays, including the adsorbed cations, controls the amount of unfrozen water. Results indicated that cation treatments have negligible effect on the unfrozen water content of kaolinite, and minimal effect on illite, chlorite, and the heterogeneous soil. Conversely, soils that are partially or completely composed of smectite demonstrated the largest unfrozen water content when treated with Na^+ cations, and a marked reduction with the K^+ treatment. Using the results of the standard clay testing, the unfrozen water content for the natural, heterogeneous soil was estimated, which matched measured values within 4%. This suggests that the unfrozen water content of a heterogeneous soil with a known mineralogy may be approximated from a database of measured standard clay unfrozen water contents of standard clays.

Table of Contents

List of Figures

Page

List of Tables

Page

List of Appendices

Page

Acknowledgements

I would like to thank my committee chair, Dr. Darrow, for her guidance throughout this entire research project. She was the instrumental second author, providing critiques of the work and guidance for development of both articles. It was the financial support from her NSF grant that allowed me to fulfill my goal for a Masters degree. I thoroughly enjoyed participating in her research, in which I gained valuable experience, and I am proud to be a contributor to her work. I would also like to thank Dr. Akagawa for his technical contributions as a third author for the submission to the *Journal of Cold Regions Engineering*. Lastly I would like to thank my other committee members, Dr. Metz and Dr. Trainor, for their insights and opinions on the development of my research and thesis.

General Introduction and Scope of Work

The research presented herein focuses on improving our understanding of liquid water in frozen soils – or unfrozen water – and its interactions with soil particles under changing thermal conditions. The main objective of the research is to determine the fraction of unfrozen water in fine-grained, cation-treated soils using a refined pulse nuclear magnetic resonance (P-NMR) methodology. The variation of unfrozen water content with changing sub-freezing temperature plays an important role in our understanding of soil freezing phenomena. For example, a precise unfrozen water content value is necessary to calculate the volumetric heat capacity and thermal conductivity of soils, which are necessary for engineering design in frozen ground (Patterson and Smith 1980). Most thermal models used to predict frozen soil behavior rely on a temperature-dependent function of unfrozen water content (Krahn 2004; and Marchenko et al. 2008) that has a great influence on the sensitivity of the model results for clayey soils (Darrow 2011). Understanding how soils' chemical and physical characteristics affect the amount of unfrozen water at a given temperature allows scientists and engineers to predict with greater accuracy how a frozen soil will behave.

In the Arctic and sub-Arctic, the presence of permafrost is common and can be problematic due to its sensitivity to changes in air temperature, or from thermal changes due to construction. Ice is the main bonding factor in permafrost soils, which gives the soils strength; however, this becomes complicated when unfrozen water films surround the soil particles (Johnston et al. 1981). Cyclic freezing and thawing can cause mechanical strength changes in soil depending on unfrozen water content (Tice et al. 1989), resulting in consolidation. In temperate regions frozen soils can adversely affect utilities, structures, and embankments through frost heaving. Frost heaving occurs in fine-grained soils as a temperature-induced pressure gradient draws water to the freezing front, forming ice lenses in the soil. Films of unfrozen water are the avenues for water migration within the freezing fringe (Torrance and

Schellekens 2006), which has been demonstrated through experiments by Akagawa (1988), Lai et al. (2014), and Zhang et al. (2014), Zhou et al. (2014), among others. This causes foundations to crack or separate, and piles to be pushed upwards, directly affecting the integrity of the overlying structure (Ferrians et al. 1969). Unfrozen water is the key factor in the behavior of frozen soil and the geologic hazards associated with it.

The research presented here is part of a larger study to measure the mass and mobility of unfrozen water in frozen soils. This research focuses on the application of pulse nuclear magnetic resonance (P-NMR) for measuring unfrozen water content within frozen soils based on the free induction decay (FID) signal intensity (SI) produced by the liquid water fraction. This thesis consists of two papers intended for publication in peer-reviewed journals. The paper presented as Chapter 1 details improvements made to the P-NMR testing method, including refinements in the laboratory set up and testing procedure. Traditionally, unfrozen water content is calculated using first return data from the FID SI; however, this data may contain both ice and liquid water responses, thus overestimating unfrozen water. This chapter includes a comparison of results obtained using traditional first return data and the normalization method, and validation of the normalization method via results obtained from two different P-NMR laboratories and a reproduction of Tice et al.'s (1982) desorption experiment.

The paper presented as Chapter 2 uses the improved P-NMR testing methodology to determine the unfrozen water content of cation-treated samples at various sub-freezing temperatures. Results from previous research have indicated that the physicochemical nature of clays, including the adsorbed cations, strongly controls the amount and mobility of unfrozen water (e.g., Grim 1952; Lambe 1953; Lambe et al. 1969; Nersesova and Tsytovich 1963). This chapter presents the unfrozen water measurements of five standard clays and one heterogeneous soil, each prepared into a suite of the untreated soil and four cation treatments.

The results from the unfrozen water measurements of the standard clays are used to predict the unfrozen water content of a heterogeneous soil containing similar components.

The findings from each chapter are combined into the General Conclusions. Appendix A contains additional figures that illustrate the cooling trends in unfrozen water content from the cation-treated samples; graphs containing warming trends are presented in Chapter 2. Finally, Appendix B contains figures containing graphs of measured hysteresis between warming and cooling trends of the standard clays and heterogeneous soil that are additional to those presented in Chapter 2.

Chapter 1 Improvements in Measuring Unfrozen Water in Frozen Soils Using the Pulse Nuclear Magnetic Resonance (P-NMR) Method[1]

1.1 Abstract

The pulse-nuclear magnetic resonance (P-NMR) method is commonly used to determine unfrozen water content in frozen soils. Traditionally, unfrozen water content is calculated using first return data from the free induction decay (FID) signal intensity (SI); however, this data may contain both ice and liquid water responses, thus overestimating unfrozen water. To address this, the authors used the "normalization method" for calculating unfrozen water. First, the authors refined a P-NMR testing system for greater temperature control. Next, testing using two P-NMR instruments at different facilities yielded repeatable unfrozen water measurements to within 2.6% of each other. Results from a desorption test indicated excellent agreement (within 1.4%) between P-NMR-derived unfrozen water and physical gravimetric water content data. Finally, comparing results from the normalization method to the first return data indicated that calculated unfrozen water in a frozen soil is up to 3.3 times greater for a given temperature using the first return data versus the normalization method. Because this difference is significant, the authors recommend further investigation using an independent method to confirm the results.

[1] Kruse, A. M., Darrow, M. M., and Akagawa, S. "Improvements in measuring unfrozen water in frozen soils using the pulse nuclear magnetic resonance (P-NMR) method." Prepared for and submitted to the *Journal of Cold Regions Engineering*.

1.2 Introduction

A key element of fine-grained frozen soils is unfrozen water, i.e., water that remains liquid at below-freezing temperatures. The unfrozen water content and mobility play key roles in frost heaving, and the thermal regime and strength of permafrost (Arenson and Sego 2006; Darrow 2011; Konrad and Morgenstern 1983; O'Neill and Miller 1985; Romanovsky and Osterkamp 2000). Thus, it is important to measure unfrozen water content accurately to facilitate engineering design in cold regions.

Anderson and Tice (1973) summarized a variety of techniques for measuring unfrozen water content in frozen soils, which included the pulse nuclear magnetic resonance (P-NMR) method. Research in the 1970s and 1980s demonstrated the suitability of the P-NMR technique for frozen soils (Kiselev et al. 1973; Kvlividze et al. 1978; Smith and Tice 1988; Tice et al. 1978, 1982; Tice and Oliphant 1984); more recently, Ishizaki et al. (1996), Tian et al. (2014), and Watanabe and Wake (2009) have used the P-NMR method to determine characteristics and quantity of unfrozen water in frozen soils.

The P-NMR method is based on characteristics of elementary particles present in all matter. All nuclei have a positive charge and many atoms have nuclei that "spin". It is the combination of spin and charge that creates a magnetic moment (i.e., a dipole). When a magnetic field is induced around these spinning particles they align themselves in the direction of the field. The strength of the magnetic field and type of nuclei (e.g., hydrogen, carbon, etc.) determines the frequency in which the nuclei align their axis of rotation in a conical sweep. When a secondary magnetic field is applied in the form of a radio frequency (RF) pulse at a right angle to the primary field, the spins resonate and absorb energy. This induces a transition between the neighboring energy levels by absorption or emission of a proton (Ruan and Chen 1998). The magnetization of nuclei may be manipulated by pulses of RF energy at intervals long enough to cause a 90° rotation of the precession angle. This is known as a 90° pulse, which is commonly used because it has the strength and duration to produce a P-NMR signal

that is proportional to the net magnetization in the X-Y plane (Callaghan 1991). When a sample is subjected to a 90° pulse, the spins will precess at different rates depending on their transition. As time continues the spins will propagate into the X-Y plane until the net magnetization is equal to zero. The decay rate of the net magnetization is known as the free induction decay (FID) (Belton 1984).

Since the establishment of the P-NMR method, unfrozen water content has been calculated using the first return values of the FID signal intensity (SI). This is the signal generated after a 90° pulse (see Figure 1.1 for a graphic illustrating the FID signal decay process and points of interest along the curve). To prevent damage to the receiver within the P-NMR instrument, a dead time is used after the pulse transmission before the coil begins to receive the FID signal; the dead time may be instrument-dependent but is typically on the order of 10μs. The first return value is the largest SI of the FID after the coil begins to receive the signal.

It is commonly assumed that the FID signal is produced only from liquid water, since the FID of ice is very fast. For example, Tice et al. (1978) assumed that the first pulse amplitude was directly proportional to the total water content, and used the first return of the FID for unfrozen water content determination; however, these authors indicated: "…we do not yet know what part of the first pulse amplitude signal from the soil ice is actually due to unfrozen water at the ice/water interface… (Tice et al. 1978)." More recently, Watanabe and Wake (2009) determined that, according to P-NMR theory, ice within soil can produce an FID signal up to 50μs. These findings call into question the accuracy of unfrozen water measurements made and calculated using the first return of the FID, as it may contain responses from both ice and liquid water, thus overestimating the unfrozen water content.

Akagawa et al. (2012) used an alternative means of calculating the unfrozen water content from P-NMR data, which herein is referred to as the "normalization method." The normalization method is based on two key findings: 1) that the FID SI is directly proportional to

the amount of unfrozen water in frozen soil (Tice and Oliphant 1984); and 2) that the ratio between the FID SI at any sub-freezing temperature and the SI at an above-freezing reference temperature must be constant (Akagawa et al. 2012). In the normalization method, all FID data are normalized to the reference-temperature FID data. The SI at the point where the normalized FID curves are horizontally parallel is used to calculate the unfrozen water content; this time is later (e.g., 60μs) than the typical first return signal.

In this paper, the authors present improvements to the P-NMR method, including refinements in the laboratory set up and testing procedure, and a comparison of results obtained using the traditional first return data and the normalization method. To provide additional validation of the P-NMR method, the authors 1) compare results from two different P-NMR laboratories (one at the University of Alaska Fairbanks (UAF), and one at Hokkaido University), and 2) repeat Tice et al.'s (1982) desorption experiment.

1.3 Materials and Methods

1.3.1 Laboratory Equipment

At the UAF location, a Maran Ultra 23MHz P-NMR instrument with a variable temperature (VT) probe was used for this research. It is housed within a modified commercial-sized refrigerator that serves as the environmental chamber (Figure 1.2). Refrigerator modifications include: inner Plexiglas doors fitted with box gloves, an Omega proportional-integral-derivative (PID) thermostat control, and platinum resistance temperature detectors (RTDs). The modified refrigerator maintains excellent thermal stability at a set point of 2°C $\pm$0.07°C, which is an advantage over cold rooms in which temperatures may fluctuate up to 5°C (Mageau and Sherman 1983). Box gloves allow for easy manipulation of samples from the remote thermal bath to the VT probe without opening the doors and compromising the thermally stable environment.

Inside the refrigerator, the P-NMR is housed in a 5-cm thick expanded polystyrene insulated foam box, with a window to monitor magnet temperature and an access port for the VT probe. The P-NMR's magnet must operate at +40.0°C to prevent detuning from the VT probe, as recommend by the manufacturer (Stevens 2004). Tice et al. (1978) and Tice and Oliphant (1984) found that this juxtaposition of measuring samples at subfreezing temperatures while maintaining magnet thermal stability was a problem for the P-NMR method, with lower environmental temperatures causing detuning of the probe. In the configuration presented here, the insulated box provides the thermal barrier necessary for magnet temperature stability (i.e., +40.0°C ±0.01°C), while the VT probe maintains the desired test temperature.

A thermal bath for sample storage is housed adjacent to the P-NMR within the refrigerator. The temperatures of the VT probe and storage thermal bath are controlled independently by two refrigerated circulating baths (RCB) outside the refrigerator, each having a variance of ±0.02°C from the given temperature set point. Each RCB is filled with a 60:40 ethylene glycol-water mixture, which is circulated into the refrigerator through insulated tubing. Condensation within the VT probe and P-NMR is prevented by flowing ultra-high pure nitrogen gas through the VT probe and P-NMR housing. The nitrogen gas first passes through a desiccator and is precooled before entering the refrigerator. Temperatures are measured using RTDs that are accurate to ±0.02°C. Two RTDs are placed into dummy soil samples within Teflon perfluoroalkoxy alkanes (PFA) resin test tubes; one test tube is located in the remote sample bath and the other is placed in the VT probe in between P-NMR measurements, for accurate temperature measurements of each location. A third RTD is located in the refrigerator chamber within a radiation shield to monitor the temperature of the overall testing environment.

1.3.2 Normalization Methodology

Figure 1.3 contains a graph of a typical FID SI from which the normalization equation is derived. Using two FID SI for thawed conditions (for this example, 5°C (FID_5) and 10°C (FID_{10})),

and their corresponding temperatures (T_5 and T_{10}, respectively), we can find the slope to determine points along the line labeled FID_x for a given temperature for which the sample is tested (T_x):

$$FID_x = \left(\frac{FID_{10} - FID_5}{T_{10} - T_5}\right) T_x + \left(\frac{FID_5 * T_{10} - FID_{10} * T_5}{T_{10} - T_5}\right) \quad \text{Eq. 1}$$

Employing Eq. 1 for the entire FID curve normalizes it to an above-freezing reference temperature FID curve. The SI at the point where the normalized FID curves are horizontally parallel is used to calculate the unfrozen water content. Figure 1.4 illustrates steps in the process; the initial FID SI (Figure 1.4a) is normalized to the known thawed reference temperature at 5°C (Figure 1.4b). The time at which all the curves are parallel is indicated by the vertical dashed line (Figure 1.4b), which in this case is 60μs. The unfrozen water content (w_u) then is calculated using the normalized FID SI at 60μs (FID_{x60}), the normalized FID SI at the reference temperature (FID_5; which, for this example, is equal to 1 (see Figure 1.4b)), and the sample's gravimetric water content (w_g):

$$w_u = \frac{FID_{x60} * w_g}{FID_5} \quad \text{Eq. 2}$$

1.3.3 Desorption Methodology

To provide an additional check on the accuracy of the P-NMR instrument and method, the authors repeated Tice et al.'s (1982) desorption experiment. This experiment originally was designed to observe the unfrozen water phase in frozen soils and its relationship to the ice phase. Anderson et al. (1978) reasoned that the total water content (w) of frozen soil consists of two components:

$$w = w_u + w_i \quad \text{Eq. 3}$$

where w_u is the unfrozen water content and w_i is the ice content. They proposed that evaporation or sublimation of a frozen sample's total water content can only be accomplished by reducing its ice content first. As the ice content reduces to zero, the total water content equals the unfrozen water content:

$$w = w_u \quad \text{Eq. 4}$$

To test this hypothesis, Tice et al. (1982) placed a desiccating molecular sieve material (MSM) above the frozen soil while measuring its unfrozen water content with a P-NMR device. As water was removed from the sample by the MSM, the unfrozen water content initially remained consistent at the expense of the ice content (Tice et al. 1982). For the current study, the desorption experiment was repeated with the P-NMR system at UAF to validate the instrument parameters and testing procedure, and to verify the accuracy of the unfrozen water content values calculated using the normalization method.

1.3.4 Sample Preparation

All samples were prepared from kaolinite clay (KGa-1b) obtained from the Source Clay Repository. Three samples were prepared for the normalization experiment. The soil was mixed to a gravimetric water content of 100% (or about twice the liquid limit) using distilled, deionized water (Figure 1.5a), and stored in a sealed container to equilibrate for two days. Three samples were made from the soil slurry: an unconsolidated sample, and two samples consolidated at 27 and 87kPa. The samples were consolidated in a modified cell (Figure 1.5b), in which filter paper was placed at the top and bottom to prevent soil loss. Once prepared, each sample was flash-frozen using liquid nitrogen (Figure 1.5c), and placed into a Teflon test tube sealed with a plastic stopper. All samples were stored in a freezer at -20°C until testing.

For the desorption experiment, the soil was mixed with distilled, deionized water to a gravimetric water content of 20.4%, and placed into a sealed beaker for five days to allow moisture equilibration. After five days, a sample was prepared inside a Teflon test tube by gently tamping the soil to achieve a density of 1.72g/cm^3 and a height of approximately 4.1cm. A small piece of filter paper was placed at the top of the sample within the test tube to prevent soil loss during MSM replacement, the test tube was capped with a stopper to form an air-tight seal (Figure 1.5d), and placed in the remote bath within the modified refrigerator to equilibrate.

1.3.5 Laboratory Testing Procedure

The modified refrigerator, RCBs, and P-NMR were turned on and given 24h to reach their designated set points and thermal equilibrium. Once equilibrated, the authors performed a calibration of the P-NMR to ensure accuracy. A sample of mineral oil was used to calibrate the P-NMR's offset, 90° pulse length, and dwell time using automated calibration functions provided within the operating software. Additionally, a sample of wet montmorillonite was used to determine the maximum receiver gain and relaxation delay, because water within the soil has a longer spin-lattice relaxation time compared to that of oil. This identified the maximum receiver gain and minimum relaxation delay that could be used in the testing, which improved the FID and reduced noise (Oxford Instruments 2006).

For the normalization test, samples were taken from the storage freezer, placed into the remote sample bath inside the modified refrigerator, and allowed to equilibrate for twelve hours at -20°C before testing. Each test tube and its sample within was taken from the bath, quickly wiped dry, and placed into the probe and tested. This procedure took approximately 30s to complete, with the samples demonstrating negligible warming (<0.06°C). Measurements were made at -20, -10, -7.5, -5, -3, -1, and -0.5°C. After each change in temperature, samples were allowed to equilibrate for 2h. After the FID signals were obtained for the suite of sub-freezing temperatures, the samples were thawed and FID signals were obtained for 5°C and 10°C. This suite of test data acquired at the UAF laboratory is referred to herein as Study A. The same soil prepared the same way was tested using the same protocol at Hokkaido University in Japan. The Japanese study is referred to as Study B; it also used a Maran Ultra P-NMR instrument, but without the VT probe.

For the desorption test, the VT probe and remote sample bath were initially set to 10°C and the sample was placed directly into the remote sample bath to equilibrate for 24h. As with the normalization test, the sample within the Teflon test tube was taken from the bath, quickly wiped dry, and placed into the probe and tested. The temperature of the system was changed

to 5°C, and after equilibrating for 1h, a second FID reading was taken. The temperature of the system then was set to -1.0°C for the remainder of the desorption test. After the initial sub-freezing measurement, 12g of MSM were poured into the test tube on top of the soil and the tube was sealed and returned to the remote bath. Several P-NMR tests were made on the sample throughout the day to record the FID SI. Every 24h the MSM was replaced, and dried in a convection oven at 150°C for 24h to determine gravimetric moisture content. This procedure was repeated for just over 300h.

While the MSM material pulled moisture from the total volume of soil (prepared to a final height of 4.1cm), the detector coil within the VT probe only detected the lower 3.5cm of the sample (determined using an incremental testing procedure developed by Tice et al. (1982)). The final gravimetric moisture content data from the MSM material were adjusted by a correction factor to account for this 15% difference in volume.

1.4 Results

1.4.1 Normalization Data Analysis

Using the normalization method, the authors determined that a time of 60μs was the earliest at which the FID SI curves were horizontally parallel to each other, thus indicating unfrozen water and not ice. Unfrozen water content then was calculated from FID signal intensity at 60μs using the gravimetric water content obtained from the samples after testing. A similar procedure was conducted using the SI at 80μs to investigate what affect using a later time would have on the calculated results. Figures 1.6a through 1.6c contain the final unfrozen water content curves produced using the normalization method at 60 and 80μs from Studies A and B. The difference in unfrozen water content at temperatures lower than -3°C for all loading conditions is less than 0.3%. The difference between values from Studies A and B increases to 2.6% at the near-freezing temperatures; this is attributed to small differences in the initial water contents of the samples in Studies A and B during preparation. These minor differences in

unfrozen water content indicate the repeatability of the P-NMR method, even from different testing facilities.

Figures 1.6d through 1.6f are comparisons of the unfrozen water contents from only Study A determined using the normalization method and the traditional first return data from the FID for the three different loading conditions. The unfrozen water contents calculated from the 60 and 80μs normalization data differ by less than 1.4%, while the first return data indicate unfrozen water contents up to 3.3 times greater for a given temperature.

1.4.2 Desorption Data Analysis

Results from the desorption test demonstrate a steady reduction in the sample's water content over the 300-h long test, with a final gravimetric moisture content of 6.2% (Figure 1.7). The average difference between the unfrozen water content determined using the FID SI at 80μs and the overall moisture content from the desorption method is 0.33%, with minimum and maximum differences of 0.17% and 1.37%, respectively. The variance observed between the two methods in Figure 1.7 is attributed to random error from humidity changes in the lab. These desorption test results validate the reliability of the P-NMR and normalization method for determining unfrozen water content.

One aspect of the desorption test that the authors expected to see was the reduction of unfrozen water at the expense of ice, as proposed by Anderson et al. (1978) and as demonstrated by Tice et al. (1982). Results indicate that there was no ice present within the sample at -1.0°C. Instead there was a steady decrease in unfrozen water throughout the testing period. The difference between the current study's results and that of Tice et al. (1982) may be attributed to the different clays used in the two experiments.

1.5 Conclusion

The refinements made to the P-NMR testing system, including using a modified refrigerator for the testing environment, an insulated box to maintain the operating temperature

of the magnet, and a P-NMR with a VT probe, provided excellent temperature control of the tested samples, thereby improving the accuracy of the measurements. The results presented here demonstrate repeatability of the P-NMR method using two different instruments and testing facilities. Results from the desorption test indicate excellent agreement between P-NMR-derived unfrozen water content values and physical gravimetric water content data, further validating the P-NMR and normalization methods. The results also indicate that the calculated amount of unfrozen water in a frozen soil for a given sub-freezing temperature varies dramatically, depending on what time after the 90° pulse is chosen for the calculations. The first return data, which has been used traditionally for these calculations and may be instrument-dependent, also may include the signal from ice yielding a significant overestimate of unfrozen water content. The normalization method presented here yields consistent results using FID signal intensity from both 60 and 80μs. Based on this data, we recommend choosing a consistent time after the 90° pulse (such as 80μs) to perform the normalization method to calculate unfrozen water content. This eliminates any variation that may be specific to the dead time required for a certain P-NMR instrument, and also removes the risk of inadvertently reading the FID signal from ice within the soil pore space. Because the difference in unfrozen water content determined from the traditional first return and normalization methods is significant, the authors recommend further investigation including comparing P-NMR results to those obtained using other methods, such as time domain reflectometry (TDR) or differential scanning calorimetry (DSC).

1.6 Acknowledgments

The authors thank Y. Miao for his many hours spent working on the temperature stability of the P-NMR system. This research was supported by the National Science Foundation under Grant Number 1147806.

1.7 Disclaimer

The views, opinions, findings, and conclusions reflected in this paper are the responsibility of the authors only and do not represent the official policy or position of the NSF, or other entity.

1.8 Figures

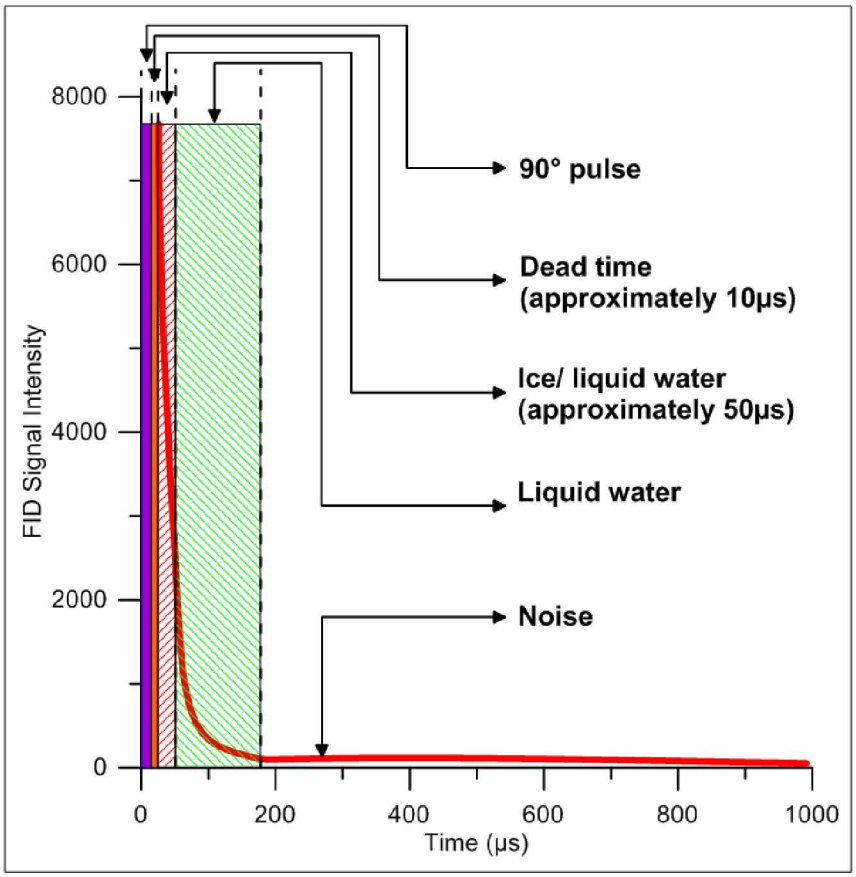

Figure 1.1 FID signal decay process and points of interest along a typical curve.

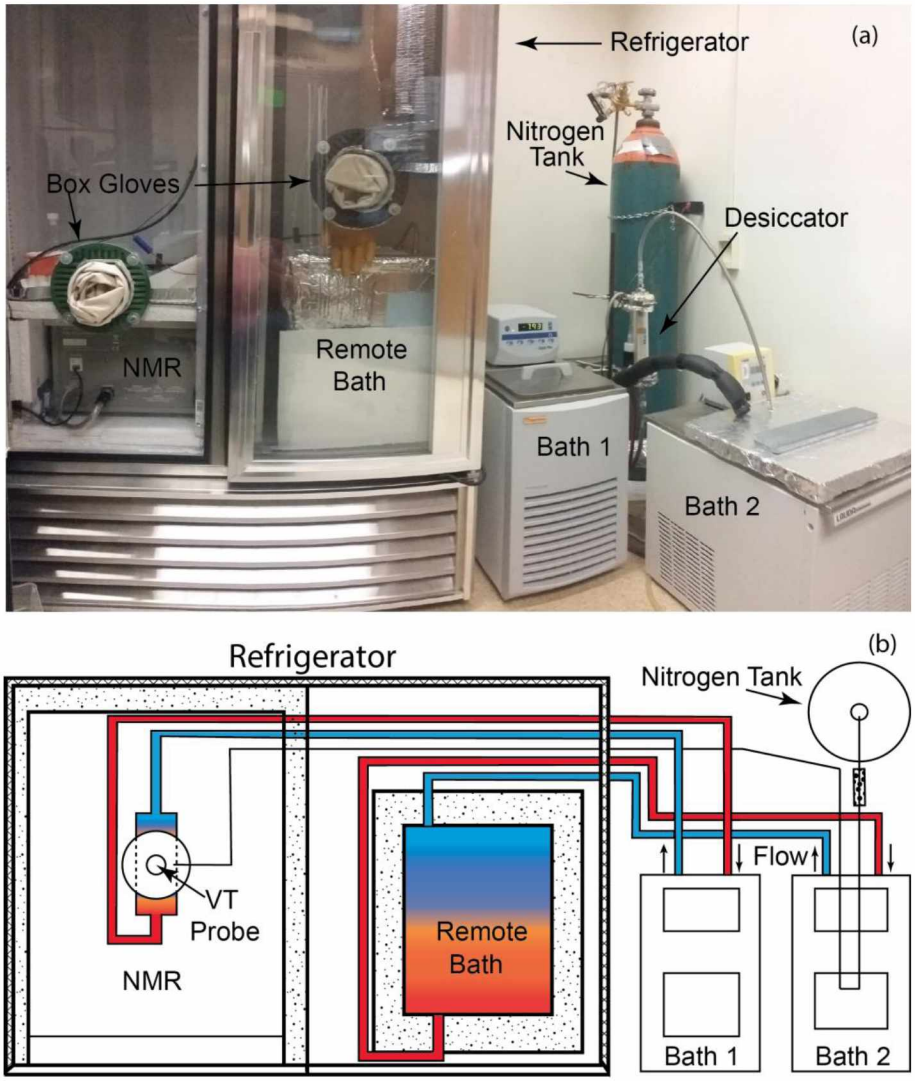

Figure 1.2 Laboratory equipment used for unfrozen water content measurement: (a) annotated photograph of equipment; (b) plan view schematic illustrating fluid flow from external thermal baths and nitrogen gas.

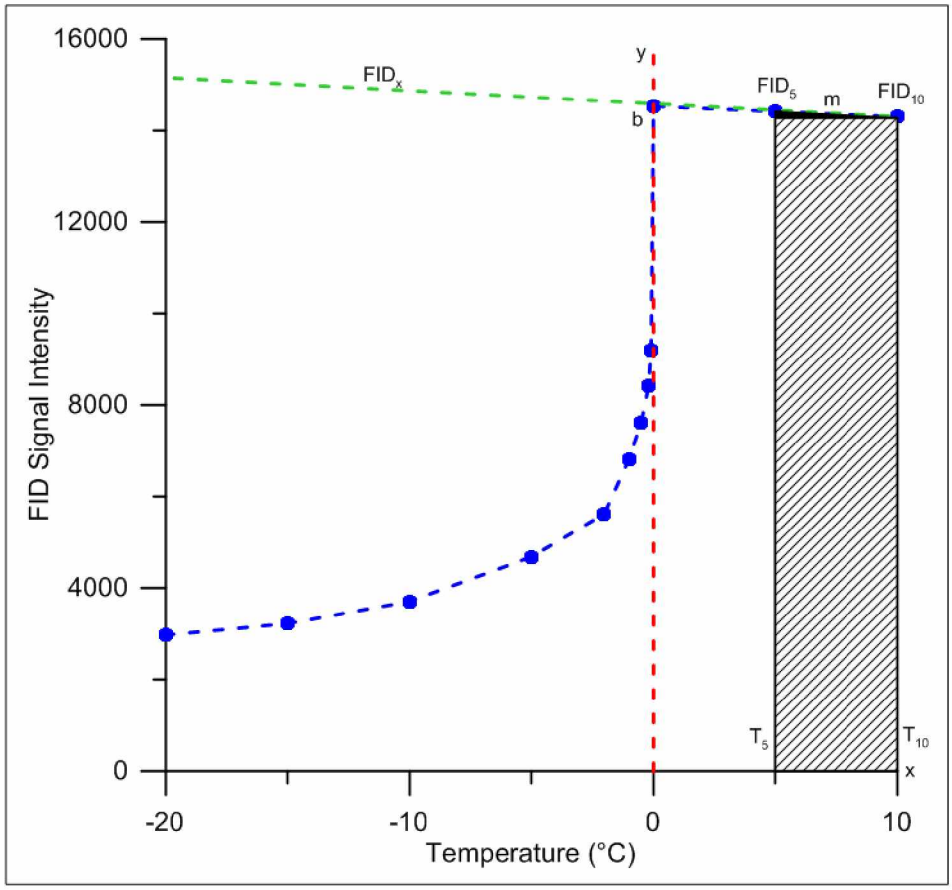

Figure 1.3 Typical P-NMR results used as a basis for calculating an FID's SI. The letter 'm' represents the slope of the line, and 'b' represents the y-intercept.

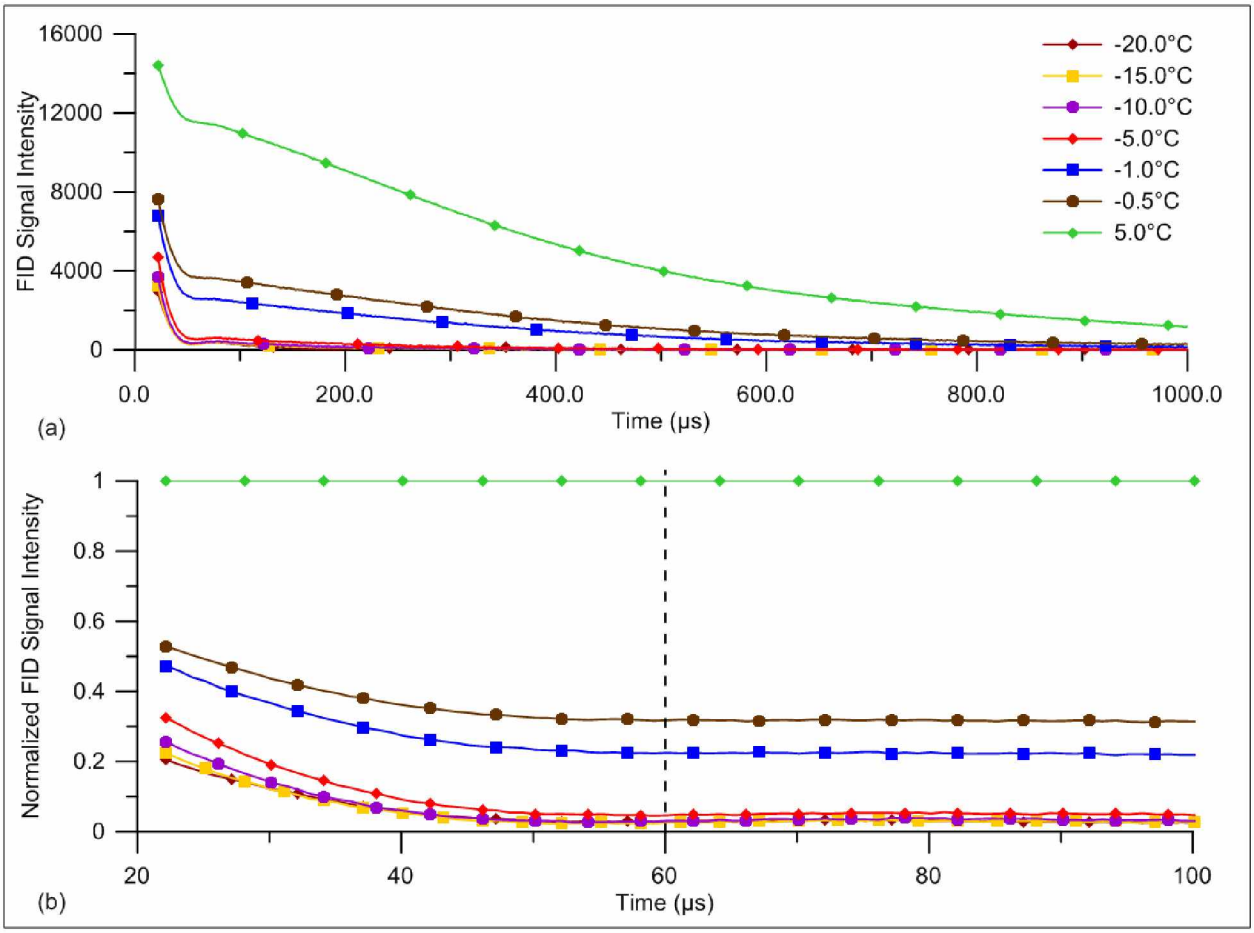

Figure 1.4 Initial FID SI over range of temperatures (a), and normalized FID SI (b). Dashed line indicates time at which all FID SI are parallel to reference temperature.

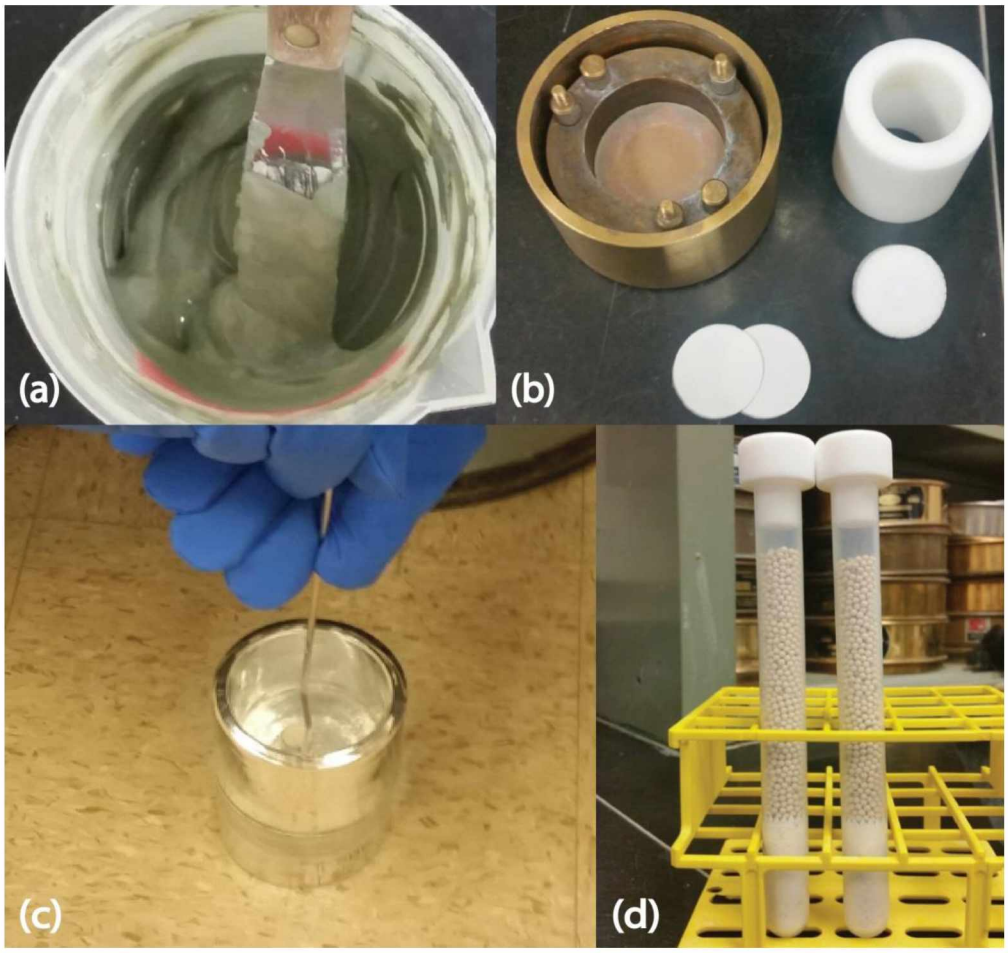

Figure 1.5 Images of sample preparation: (a) soil slurry prepared to 100% gravimetric moisture content; (b) modified consolidation cell with plunger (white ring and plug) placed inside original loading cell with filter paper placed at top and bottom of soil slurry; (c) sample is flash frozen inside Dewar containing liquid nitrogen; (d) consolidated kaolinite samples (bottom) with MSM material (top) for the desorption test.

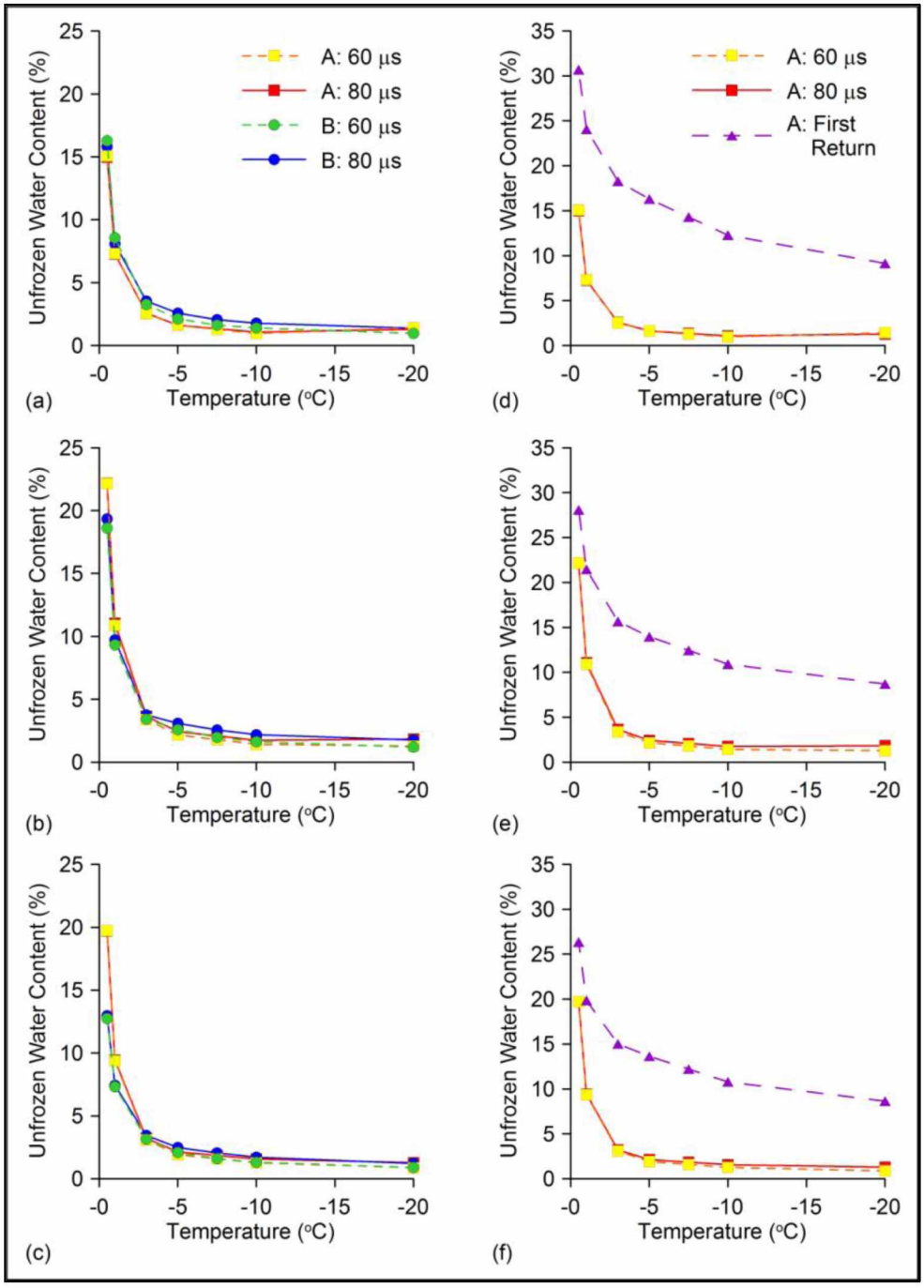

Figure 1.6 Comparison of unfrozen water content curves from Studies A and B (a, b, c) and using the first return data versus the normalization method (d, e, f). Results are shown for an unconsolidated sample (a and d), and samples consolidated at 27 kPa (b and e), and 87 kPa (c and f).

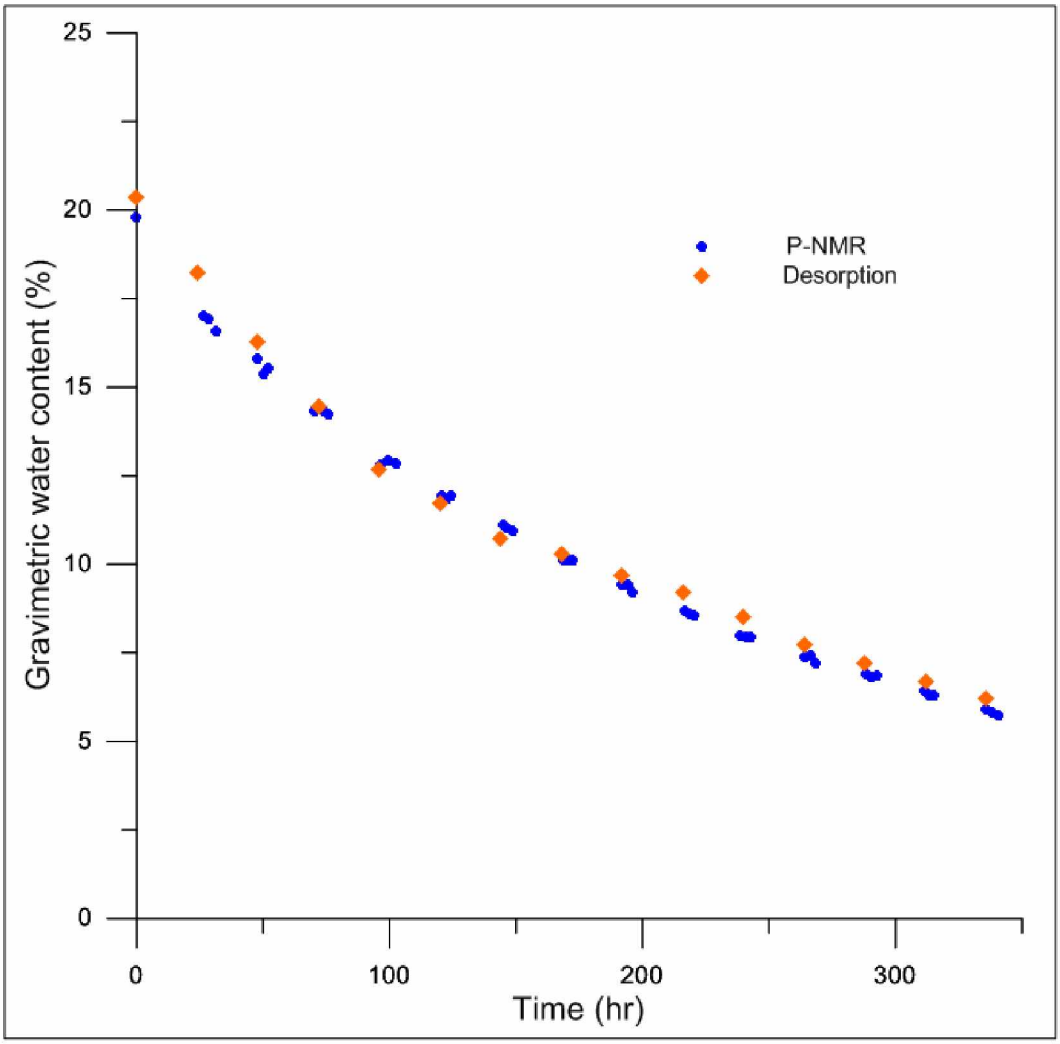

Figure 1.7 Comparison of P-NMR-calculated gravimetric unfrozen water content and water content determined via desorption.

1.9 References

Akagawa, S., Iwahana, G., Watanabe, K., Chuvilin, E. M., Istomin, V. A. (2012). "Improvement of pulse NMR technology for determination of unfrozen water content in frozen soils." *Tenth International Conference on Permafrost, International Contributions:* The Northern Pub., Severnoye Izdatelstvo, Russia, 1, 21-25.

Anderson, D. M., Pusch, R., Penner, E. (1978). "Physical and thermal properties of frozen ground." In Andersland, O. B., and Anderson, D. M., eds., *Geotechnical Engineering for Cold Regions*, McGraw-Hill, New York, NY, 37-102.

Anderson, D. M., and Tice, A. R. (1973). "The unfrozen interfacial phase in frozen soil water systems." In *Ecological Studies: Analysis and Synthesis*, 4, 107-124.

Arenson, L. U., and Sego, D. C. (2006). "The effect of salinity on the freezing of coarse-grained sands." *Canadian Geotechnical Journal*, 43, 325-337.

Belton, P. S. (1984). "Spectroscopic methods: nuclear magnetic resonance and photoacoustic spectroscopy." In Chan, H. W. S, Ed*., Geophysical Methods in Food Research,* Blackwell Scientific Pub, Boston, Mass., 106-119.

Callaghan, P. T. (1991). *Principles of Nuclear Magnetic Resonance Microscopy*: Oxford University Press, New York, N.Y.

Darrow, M. M. (2011). "Thermal modeling of roadway embankments over permafrost." *Cold Regions Science and Technology*, 65, 474-487, doi:10.1016/j.coldregions.2010.11.001

Ishizaki, T., Maruyama, M., Furukawa, Y., Dash, J. G. (1996). "Premelting of ice in porous silica glass." *Journal of Crystal Growth*, 163, 455-460.

Kiselev, V. F., Kvlividze, V. I., Kurzayev, A. B. (1973). "Surface phenomena at the ice-gas and ice-solid interfaces." *Proc., Permafrost; Second International Conference, USSR Contribution*, National Research Council of Canada, National Academy of Science, Yakutsk, U.S.S.R., 339-341.

Konrad, J. M., and Morgenstern, N. R. (1983). "Frost susceptibility of soils in terms of their segregation potential." *Proc., Permafrost: Fourth International Conference*, University of Alaska Fairbanks and National Academy of Sciences, Fairbanks, Alaska, 660-665.

Kvlividze, V. I., Kiselev, V. F., Krasnushkin, A. V., Kurzayev, A. B., Ushakova, L. A. (1978). "An NMR study of the phase transition of water in models and in frozen clays." *Third International Conference on Permafrost*, National Research Council of Canada, Edmonton, Alberta, Canada. Trans. (1980). *English Translations of the Forty-Nine Soviet Papers, and the One French Paper, and the Three Invited Soviet Theme Papers: Proc., Third International Conference on Permafrost*, National Research Council of Canada, Edmonton, Alberta, Canada, 1, 81-96.

Mageau, D. W., and Sherman, M. B. (1983). "Frost cell design and operation." *Proc., Permafrost: Fourth International Conference, University of Alaska Fairbanks,* National Academy Press, Washington, D.C., 767-772.

O'Neill, K., and Miller, R. D. (1985). "Explorations of a rigid ice model of frost heave." *Water Resources Research*, 21(3), 281-296.

Oxford Instruments. (2006). *MARAN Ultra Non-Expert User Manual*: Oxford Instruments Ltd., Tubney Wood, Abingdon, UK.

Romanovsky, V. E., and Osterkamp, T. E. (2000). "Effects of unfrozen water on heat and mass transport processes in the active layer and permafrost." *Permafrost and Periglacial Processes*, 11, 219-239.

Ruan, R. R., and Chen, P. L. (1998). *Water in Foods and Biological Materials*: *Nuclear Magnetic Resonance Techniques*: Technomic Publishing Company, Inc., Lancaster, PA, 1-50.

Smith, M. W., and Tice, A. R. (1988). *Measurement of the Unfrozen Water Content of Soils*: CRREL Report 88-18, US Army Cold Regions Research and Engineering, Hanover, NH.

Stevens, G. (2004). *MARAN Ultra Service Manual*, Oxford Instruments Ltd., Tubney Woods, Abingdon, UK.

Tian, H., Wei, C., Wei, H., Zhou, J. (2014). "Freezing and thawing characteristics of frozen soils: bound water content and hysteresis phenomenon." *Cold Regions Science and Technology*, 103, 74-81.

Tice, A. R., Burrous, C. M., Anderson, D. M. (1978). "Determination of unfrozen water in frozen soil by pulsed nuclear magnetic resonance." *Third International Conference on Permafrost*, The National Research Council of Canada, Alberta, Canada, 1, 150-155.

Tice, A. R., and Oliphant, J. L. (1984). "The effect of magnetic particles on the unfrozen water content of frozen soils determined by nuclear magnetic resonance." *Soil Science*, 138(1), 63-73.

Tice, A. R., Oliphant, J. L., Nakano, Y., Jenkins, T. F. (1982) *Relationship Between the Ice and Unfrozen Water Phases in Frozen Soil as Determined by Pulsed Nuclear Magnetic Resonance and Physical Desorption Data*: CRREL Report 82-15, US Army Cold Regions Research and Engineering Laboratory, Hanover, NH.

Watanabe, K., and Wake, T. (2009). “Measurement of unfrozen water content and relative permittivity of frozen unsaturated soil using NMR and TDR.” *Cold Regions Science and Technology*, 59, 34-41.

Chapter 2 Absorbed Cation Effects on Unfrozen Water in Fine-Grained Frozen Soil Using Pulsed Nuclear Magnetic Resonance[1]

2.1 Abstract

Unfrozen water within frozen soils is a key component that determines a soil's thermophysical response to changing physical and environmental conditions. The physicochemical nature of the clay component of fine-grained soils, including the adsorbed cations, strongly controls the amount and mobility of unfrozen water. Here we present the unfrozen water measurements of five standard clays and one heterogeneous soil. For each soil, we prepared a suite of the untreated soil and four cation treatments, which represents a comprehensive data set of clays and dominant cations typically found in soils. We measured unfrozen water content using a refined pulse nuclear magnetic resonance (P-NMR) testing facility and the normalization method, which yielded accurate and repeatable results. Results indicated that cation treatments have negligible effect on the unfrozen water content of kaolinite, and minimal effect on illite, chlorite, and the heterogeneous soil. Conversely, soils that are partially or completely composed of smectite demonstrated the largest unfrozen water content when treated with Na^+ cations, and a marked reduction with the K^+ treatment. From the results of the standard clay testing, we estimated the unfrozen water content for the natural, heterogeneous soil, producing curves that matched those measurements to within 4% for all cation treatments. This suggests that the unfrozen water content of a heterogeneous soil with a known mineralogy may be approximated from a database of measured standard clay unfrozen water contents of standard clays.

[1] Kruse, A. M., and Darrow, M. M. "Absorbed cation effects on unfrozen water in fine-grained frozen soil using pulsed nuclear magnetic resonance." Prepared for submission to *Cold Regions Science and Technology*.

2.2 Introduction

Unfrozen water is a thin film of liquid water that exists on the mineral surfaces in fine-grained soils at below-freezing temperatures. The amount and distribution of unfrozen water impacts frost heaving (e.g., Hoekstra 1966; Miller 1978; Torrance and Schellekens 2006; Williams 1964), mechanical properties of frozen soil, such as creep (Aksenov et al. 1998; Klein and Jessberger 1976), and the thermal regime of frozen ground (Darrow 2011; Romanovsky and Osterkamp 2000). The variation of unfrozen water content with changing sub-freezing temperature plays an important role in understanding soil freezing phenomena (Patterson and Smith 1980). In fact, several authors have stated that the presence and amount of unfrozen water is key to all thermophysical processes in freezing soils (Kozlowski 2003; Nersesova and Tsytovich 1963). This stresses the importance of accurately measuring unfrozen water for thermal modeling, and understanding its *in situ* behavior for frozen ground engineering.

Measuring unfrozen water in frozen soil began with the pioneering dilatometer work by Bouyoucos (1917, 1920). In the decades that followed, practitioners developed additional methods such as differential scanning calorimetry (DSC), time-domain reflectometry (TDR), and the pulse nuclear magnetic resonance (P-NMR) method (Anderson and Tice 1973). The P-NMR method was first developed and refined for frozen soil testing in the 1970's and 1980's (e.g., Kiselev et al. 1973; Smith and Tice 1988; Tice et al. 1978). Later experiments used the P-NMR method for further characterization of unfrozen water and its interactions within frozen soil (Ishizaki et al. 1996; Tian et al. 2014; Watanabe and Wake 2009). The method is based on the concept that many nuclei (including hydrogen) act as magnetic dipoles and align themselves within an external magnetic field. The nuclei are stimulated with a pulse of radio-frequency (RF) electromagnetic radiation (often oriented at 90°), and the RF emission produced as the excited nuclei return to their equilibrium orientations is recorded (Atkins and de Paula 2002). This RF emission is termed the free induction decay (FID). Traditionally, unfrozen water content has

been calculated using the first return of the FID signal intensity (SI), which is recorded as early as 20μs after the 90° pulse; however, this value may record both liquid water and ice content, resulting in an overestimation of unfrozen water content (Akagawa et al. 2012; Kruse et al. (in review); Watanabe and Wake 2009). To address this problem, Akagawa et al. (2012) introduced the normalization method, in which the sub-freezing FID SI is normalized to the SI at an above-freezing temperature. The unfrozen water content is calculated using the SI value at the time when the SI curves become parallel to each other (e.g., 80μs). Recent P-NMR testing demonstrated the accuracy and repeatability of this refined method (Kruse et al. (in review)).

Fine-grained soils typically consist of a range of grain sizes, with clay minerals forming the "active" portion of these soils (Taylor and Ashcroft 1972). The physiochemical nature of clays, including the adsorbed cations, strongly controls the amount and mobility of unfrozen water present (Darrow et al. 2009; Grim 1952; Hoekstra 1966; Konrad and Morgenstern 1983; Lambe 1953; Lambe et al. 1969; Nersesova and Tsytovich 1963). Thus, the clay component of a heterogeneous soil is a critical parameter influencing its frost susceptibility and strength; however, heterogeneous soils are complicated systems that make isolating the effects of each variable difficult.

As part of a larger project to investigate the mass and mobility of unfrozen water, surface charge, and micro-aggregate and micro-fabric formation in frozen cation-treated soils, here we present the unfrozen water measurements of five standard clays and one heterogeneous soil. Each soil was prepared into a suite of the untreated soil and four cation treatments (Ca^{2+}, Mg^{2+}, Na^{+}, and K^{+}). After first demonstrating repeatability of the testing system and method, we used a P-NMR device and the normalization method to determine the unfrozen water content for all samples at varying sub-freezing temperatures. The results represent a comprehensive, high-quality data set for standard clays typically found in natural soils. Using the results from the standard clays, we present a comparison of the calculated unfrozen water content of the

heterogeneous soil to its measured unfrozen water content. These results have implications on how an *in situ* heterogeneous soil may be affected by natural cation exchange.

2.3 Overview of Clay Mineralogy and Surface Charge

For this research, we tested five clays that are commonly found in soils: kaolinite, montmorillonite, illite, illite-smectite, and chlorite (Lambe 1953). Although available in general texts on soil mineralogy, we present a brief overview of clay mineralogy as it pertains to this research. Clays are phyllosilicate minerals composed of sheets of silica tetrahedra and aluminum octahedra (Tan 1998). The electronegative charges on clay particles that result in surface cation exchange are due to isomorphic substitution and, to a lesser extent, the dissociation of exposed hydroxyl groups. For example, the replacement of Si^{4+} with Al^{3+} in the tetrahedral layer will result in a net negative charge. Similarly, Al^{3+} may be replaced by Mg^{2+} in the octahedral sheet without disturbing the crystal structure. The size and valence of the ions determines the ease with which isomorphic substitution takes place (Tan 1998). Additionally, the dissociation of H^+ from OH^- groups on the particles' edges forms a pH-dependent charge.

Kaolinite is a 1:1 phyllosilicate mineral that typically has a small net negative charge (Tan 1998). The layers are held together tightly by hydrogen bonding between the O^{2-} and OH^- ions giving kaolinite a small specific surface area (SSA) and cation exchange capacity (CEC). For this reason kaolinite interlayer surfaces do not tend to separate giving this clay a low swelling capacity (McBride 1994).

The smectite group consists of expanding 2:1 layer clays that have the structure of one aluminum octahedral sheet sandwiched between two silica tetrahedral sheets. The negative charge of montmorillonite (a member of the smectite group) is attributed to Mg^{2+} and Fe^{3+} ions replacing Al^{3+} in octahedral positions, which contributes to its large CEC (Tan 1998). Within the interlayers, weak electrostatic attractive forces hold the layers together; however, the swelling

capacity of this mineral group differs depending on the type of adsorbed surface cation, which affects the electrostatic potential and the SSA (Macht et al. 2011; McBride 1994; Tan 1998). In some cases, the interlayer swelling can double the mineral's volume (Tan 1998). Generally, the minerals of the smectite group exhibit high plasticity and stickiness when wet because of their large surface areas.

Illite is a nonexpanding 2:1 layer clay, which forms as a secondary mineral from micaceous minerals, and thus has a similar structure to its parent minerals. Several authors object to classifying illite as a clay, and instead suggest it should be referred to as a clay-sized mica (Fanning and Keramidas 1977; Theng 1972). This is due to how closely its chemical composition resembles muscovite; however, illite contains more SiO_2 and less K^+ due to weathering processes. Because of this close relationship to mica, illite has been identified as hydrous mica or soil mica (Tan 1998). Substitution of Al^{3+} for Si^{4+} in the tetrahedral layer creates a net negative charge; however, K^+ cations in the interlayers tightly bind the layers together, which reduces the SSA and creates an irreversibly bound condition for K^+ (McBride 1994). Thus, the intermicellar spaces of illite do not expand with the addition of water, resulting in illite's low plasticity, low shrink-swell capacity, and low CEC as compared to smectite (Tan 1998). The illite-smectite clay used in this research is a 70/30 mix with low expandability (Geramian et al. 2016). Its mix of both clay species, however, gives it the second largest CEC and SSA of the tested samples (Table 2.1).

Chlorite is a 2:2 layer clay, consisting of a hydrated magnesium octahedral sheet sandwiched between two silica tetrahedral sheets, which are bound together by an interlayer brucite sheet. Isomorphic substitutions occur in both tetrahedral and octahedral layers, in which Si^{4+} is replaced by Al^{3+}, and Mg^{2+} is replaced by Fe^{3+} or Al^{3+}, respectively. A positive charge develops from the replacement of Mg^{2+} by Al^{3+} in the brucite sheet, which nearly neutralizes the overall negative charge (Tan 1998). Chlorite's brucite layer causes a small SSA and low CEC,

which further results in a low swelling capacity and limits cation exchange to the external surfaces of chlorite particles (McBride 1994).

The overall negative surface charge of clay minerals from isomorphic substitution and edge effects attracts positively charged ions to the particle surfaces to neutralize the charge. The most common exchangeable cations in soils are the divalent cations Ca^{2+} and Mg^{2+}, and the monovalent cations H^+, Na^+, and K^+. Hydrated cations form a swarm about the mineral surface to balance the negative charge, forming a tightly adsorbed layer called the Stern layer, and a less structured cation swarm called the Gouy-Chapman diffuse double layer (Heagler 1964; Taylor and Ashcroft 1972). The negative charge at the Stern layer is described as the zeta potential, which depends on the type of adsorbed cations. For example, divalent cations adsorbed in the Stern layer more effectively neutralize the negative charge, resulting in a less-negative zeta potential, a thinner diffuse double layer, and a thinner layer of oriented water at the mineral's surface (Grim 1958). In contrast, adsorbed monovalent cations result in a more-negative zeta potential, and thicker adsorbed water and diffuse double layers. Under sub-freezing conditions, the surface chemistry affects the unfrozen water in a similar fashion.

2.4 Materials and Methods

2.4.1 Laboratory Equipment

The P-NMR instrument used in this research is a Maran Ultra 23MHz device with a variable temperature (VT) probe. It is housed within an environmental chamber modified from a commercial-sized refrigerator (Figure 2.1). The internal refrigerator temperature is maintained by an Omega proportional-integral-derivative (PID) thermostat control and monitored using a platinum resistance temperature detector (RTD). This setup maintains excellent thermal stability at a set point of 2°C $\pm$0.07°C. Inner Plexiglas doors fitted with box gloves allow for easy manipulation of samples from a remote thermal bath located within the chamber to the VT

probe, without major thermal fluctuations from opening the doors. Within the refrigerator, the P-NMR is housed in a 5-cm thick expanded polystyrene insulated foam box, with an access port on top for the VT probe and a window in front to monitor magnet temperature. This insulated environment for the P-NMR device is necessary to maintain an operating temperature of +40°C, thus eliminating detuning of the probe caused by temperature fluctuations (Kruse et al. (in review)).

Two external refrigerated circulating baths (RCB) independently maintain temperature set points for the VT probe and the remote sample bath. Each RCB is filled with a 60:40 ethylene glycol-water mixture that is circulated into the refrigerator via insulated tubing, maintaining set point temperatures with a variance of ±0.02°C. Ultra-pure nitrogen is used to prevent condensation within the VT probe housing, first flowing through a desiccator to remove any excess moisture, and then through a coil within an RCB for precooling before entering the VT probe. Two RTDs placed into dummy soil samples within Teflon perfluoroalkoxy alkanes (PFA) test tubes are used to monitor temperatures for both the remote sample bath and the VT probe.

2.4.2 Sample Preparation

For this research, we tested five homogeneous clays obtained from the Source Clay Repository at Purdue University: montmorillonite, kaolinite, illite, illite-smectite, and chlorite (see Table 2.1 for locations of origins). We also tested a heterogeneous soil sampled from the Copper River Basin, about 5km south of Glennallen, Alaska. This soil (referred to herein as Copper River) classified as a lean clay (CL) using the Unified Soil Classification System, and Table 2.2 is a summary of its mineral components based on a semi-quantitative X-ray diffraction (XRD) analysis (conducted by K/T GeoServices, Inc.).

As some of the homogeneous clays were available only in the form of rock chips we first processed these samples to obtain silt- and clay-sized particles. This processing was not needed for the montmorillonite and kaolinite (which were ground to a powder by the mining company supplier), nor for the Copper River soil. The rock chips were soaked in distilled, deionized (DI) water (Figure 2.2a), then gently crushed with a rubber-tipped pestle and a mortar to yield particles smaller than 3mm in diameter. These particles were reduced further using a ball mill, until all particles passed through a US No. 200 (75μm) sieve (Figure 2.2b). We compared grain-size distributions produced using a hydrometer (ASTM D422; ASTM 1998) for all six soils to verify that the sample processing yielded adequate silt- and clay-sized particles for further testing. While there are variations in the grain-size distributions, the percentage of the finest particles (i.e., <0.8μm) for all of the soils processed with the mortar and pestle and ball mill are between those produced by the commercial supplier (i.e., montmorillonite and kaolinite; Figure 2.3).

Next, we prepared four cation treatments (Ca^{2+}, Mg^{2+}, Na^{+}, and K^{+}) for each of the six soils; these treatments, along with the untreated soils in their natural states, represented the 30 samples that were tested for unfrozen water. For each cation treatment, 40g of soil was mixed with 1L of a 1.05M solution of salt (e.g., $CaCl_2$, $MgCl_2$, NaCl, or KCl). The mixture was divided between two 1L plastic bottles and agitated for two days on a shaker table to ensure cation exchange. We then flushed the chloride from the soil-brine mixture using Buchner filter funnels, with filter paper placed at the base to prevent soil loss and allow for easy sample removal. Each sample was repeatedly mixed with DI water, which was pulled through the funnel using vacuum and collected below in an Erlenmeyer flask. The effluent was measured using an electroconductivity meter, and this rinsing process was repeated until the electroconductivity measured approximately 10μS. The Na^{+}- and K^{+}-treated montmorillonite, illite, illite-smectite, and Copper River soil demonstrated such low hydraulic conductivity that the DI water would not

pass through the clay in the funnel. For these samples, we removed the excess chloride through dialysis. The sample was transferred into dialysis tubing, and the ends were secured. The tubing was suspended in a 600mL beaker and submerged in DI water. The electroconductivity was measured every 24h, and the water was replaced when the electroconductivity became constant. This process was repeated until the electroconductivity was less than 20μS.

Finally, we prepared all of the untreated and cation-treated samples for P-NMR testing. Each sample was mixed into a slurry using DI water, and sealed within an air-tight container to equilibrate for a minimum of five days. The slurry was poured into a modified consolidation cell (Figure 2.2c), and consolidated at 75kPa. A coring tool (with a height of 4.0cm and inner diameter of 1.3cm) was used to core a portion of the consolidated clay, which then was slowly dipped into liquid nitrogen for flash-freezing (Figure 2.2d). After the sample was completely frozen, we pushed the soil from the coring device using a wooden dowel (Figure 2.2e), quickly wrapped the sample in plastic paraffin film, placed it into a small glass tube with a rubber-lined cap to prevent sublimation, and finally placed it within a secondary sealed container inside a freezer set at -20°C until used for testing. This process produced a cylindrical sample that spanned the entire length of the VT probe's coil. To demonstrate repeatability and accuracy of the testing system and sample preparation procedure, we separately prepared a second complete suite of kaolinite samples for P-NMR testing. Table 2.3 is a summary of the final water contents and dry densities of all the tested samples.

2.4.3 Laboratory Testing Procedure

We turned on the modified refrigerator, RCBs, and P-NMR, letting them run for 24h to reach their set temperatures and thermal equilibrium before calibrating the P-NMR. Placing a test tube filled with mineral oil within the VT probe, we ran a set of automated calibration functions provided within the software to set the P-NMR's offset, 90° pulse length, and dwell

time. Since water within soil has a longer spin-lattice relaxation time compared to mineral oil, we also set the receiver gain to a standard limit for all soil testing, which required determining the maximum value to improve the free-induction decay (FID) signal and reduce noise (Oxford Instruments 2006), without "clipping" the final signals. We used a sample of montmorillonite prepared to a gravimetric water content of 330% to determine the maximum receiver gain and relaxation delay, since it demonstrated the highest water content of all of the samples after loading (Table 2.3).

Each soil suite of five samples was taken from the storage freezer, unwrapped and transferred to Teflon test tubes, and then placed in the remote sample bath to equilibrate for a minimum of 12h at -20°C. Measurements were made over a range of warming temperatures (-20, -15, -10, -5, -2, -1, and -0.5°C) and then retested at the same set of temperatures to establish a cooling trend. To make an FID measurement, each sample was removed from the remote bath, quickly wiped dry, placed into the VT probe, and tested. This procedure took approximately 30s from start to finish with samples demonstrating negligible warming (<0.06°C). Once a new set point temperature was established within the remote bath, samples were allowed to equilibrate for an additional 2h before the next set of FID measurements. Once all the FID values were obtained for sub-freezing conditions, the samples were thawed and FID measurements were taken at 5°C and 10°C.

2.4.4 FID SI Processing

For this research, we used the normalization method (Akagawa et al. 2012; Kruse et al. (in review)) to determine unfrozen water content, in which the FID SI sub-freezing curve is normalized to an above-freezing FID SI curve. The SI at the point where the normalized FID curves are horizontally parallel is used to calculate the unfrozen water content; for this research, the unfrozen water content (w_u) was calculated using the normalized FID SI at 80μs (FID_{x80}), the

normalized FID SI at the reference temperature (FID_5, which is equal to 1), and the sample's gravimetric water content (w_g):

$$w_u = \frac{FID_{x80} * w_g}{FID_5} \quad \text{Eq. 5}$$

This method is based on two key principles: 1) the amount of unfrozen water is directly proportional to the FID SI (Tice and Oliphant 1984); and 2) the ratio between the FID SI at any sub-freezing temperature to that of the SI in a thawed condition must be constant (Akagawa et al. 2012).

2.5 Results and Discussion

2.5.1 Cation-treated Soils

Figure 2.4 is a summary of the test results for two separately prepared suites of kaolinite samples, identified as samples A and B in each sub-figure. The unfrozen water content typically differed by less than 2% between samples A and B, with a maximum difference of 2.8% at -1.0°C for all sample pairs. This difference of 2.8% close to the phase change temperature may be attributed to actual gravimetric water content measured after testing, which differed up to 2% between sample sets (Table 2.3). Overall, these separately prepared and tested samples demonstrate excellent agreement and thus accuracy of the P-NMR testing system. For the rest of the analysis, only data from the kaolinite sample set A will be used for comparison.

Figure 2.5 and Table 2.4 contain the unfrozen water content results for each suite of samples for a given soil type. Montmorillonite and illite-smectite demonstrated the largest amount and/or greatest variance of unfrozen water content (Figures 2.5a and 2.5d); this result is in agreement with previous findings (Grim 1952; Lambe 1953; Nersesova and Tsytovich 1963; Odom 1984). For these soils, the Na^+ treatment yielded a higher concentration of unfrozen water near freezing, which became closer to the other cation treatments at colder temperatures.

This high unfrozen water content for the Na^+-treated samples is attributed to their large SSAs and the swelling capacity of the smectite group. The hydratable nature of the Na^+-treated smectite produces a large diffuse double layer composed of oriented, adsorbed water that is easily supercooled (Lambe 1953; Martin 1960; Odom 1984), causing it to remain largely unfrozen at increasingly negative temperatures.

The unfrozen water content of the K^+-treated montmorillonite sample remained well below the other cation treatments throughout the entire temperature range (Figure 2.5a); this only occurred for the montmorillonite soil. Previous research conducted at Cornell University (1951) and by Grim (1952) suggested that some permanent fixation of the K^+ ion may occur within the montmorillonite crystal structure, causing very little water adsorption with a "definite configuration." This structured water in the K^+-treated montmorillonite sample may be manifested as a lower unfrozen water content.

Using the normalization method, the unfrozen water content for kaolinite differed by less than 1.5% among all of the treatments, which is manifested by the nearly identical plotted curves (Figure 2.5b). Nersesova and Tystovich (1963) had similar findings using an isothermal calorimeter. This lack of change in unfrozen water content per cation treatment is attributed to kaolinite's small SSA and CEC (Grim 1952). Likewise, no systematic differences are obvious in the trends of the other cation-treated soils, as the unfrozen water content of the various treatments differed by less than 2.5% for illite, chlorite, and Copper River.

Figure 2.6 is a comparison of the unfrozen water content by cation treatment. Montmorillonite consistently had the highest unfrozen water content for each treatment, demonstrating up to 25% more unfrozen water than illite-smectite and Copper River (with the second and third highest amounts, respectively). Chlorite and illite demonstrated the lowest unfrozen water contents, with less than 8% and 12% for all treatments, respectively. Chlorite

has both small SSA and CEC, and the brucite layer limits cation exchange to the external mineral surfaces. All of this is manifested in its extremely low unfrozen water content as compared to the other minerals.

Per treatment, the unfrozen water content trends of these soils were fairly consistent in their difference from each other. Kaolinite was the exception, crossing the trends of the other soils with unfrozen water contents up to 25% near 0°C dropping to 3% or less at -20°C. This clay's steep reduction in unfrozen water content between 0°C and -5°C may be due to its grain-size distribution and the small amount (<8%) of particles finer than 0.8μm.

2.5.2 Hysteresis

Hysteresis in frozen soils may be similar to the capillary hysteresis in wetting-drying cycles of porous media (Hillel 1998). The possible mechanisms to cause phase transition hysteresis include pore blocking and the capillary effect (both related to pore size, shape, and radius), metastable nucleation (i.e., pore water can remain in a liquid state at sub-zero temperatures), and the electrolyte effect (i.e., a depression in the freezing point due to solute concentration; Tian et al. 2014).

Although it is sometimes assumed that the unfrozen water content is the same for warming and cooling runs (Kozlowski 2003), we observed some amount of hysteresis in all of the soils tested, with the greatest amount demonstrated in the suite of montmorillonite samples (Figure 2.7). These samples typically demonstrated hysteresis over the full range of testing temperatures, experiencing as much as 4.9% difference in unfrozen water content at -2.0°C for the K^+-treated sample (Figure 2.7e). We propose that the hysteresis may be caused by structural changes that occur during the flash freezing of the sample with liquid nitrogen. As the soil is flash frozen at extremely cold temperatures (e.g., the boiling point of liquid nitrogen is -196°C), we hypothesize that micro-lenticular ice lenses may form within the soil. As the

temperature of the frozen sample rises during the warming cycle, these micro-lenticular ice lenses melt and the amount of unfrozen water increases, as expected. During the cooling cycle, however, the ice lenses do not reform, resulting in a higher unfrozen water content for the same sub-freezing temperature, i.e., hysteresis. The Na^+-treated sample, with the greatest amount of unfrozen water of all samples, demonstrated minimal hysteresis for temperatures warmer than -2°C. This suggests that this soil had less micro-lenticular ice lensing and more unfrozen water after its initial flash freezing, reducing the difference between warming and cooling runs and thus limiting the demonstrated hysteresis.

2.5.3 Estimated Unfrozen Water Content of a Simulated Soil

If the mineral composition of a heterogeneous soil is known, it may be possible to create its unfrozen water characteristics based on previous laboratory studies of various cation-treated standard clays. Curious to see if we could "build a soil" from the results of the unfrozen water content testing, we simulated the unfrozen water content of the heterogeneous Copper River soil using the semi-quantitative XRD analysis (Table 2.2) and the unfrozen water data from the source clay sample suites. As we did not test a randomly ordered mixed-layer chlorite-smectite clay, we simulated this component by adding the 70/30 mix of illite-smectite to the chlorite. Then we multiplied the individual phyllosilicate components by their corresponding source clay unfrozen water contents to produce the estimated Copper River sample. An error of ±5% was taken into consideration in this compilation to account for detection limits of the XRD analysis (K/T GeoServices, pers. comm., 2006). As seen in Figure 2.8, the simulated soil's unfrozen water content has similar trends to its real counterpart. The largest variance occurs at temperatures higher than -2°C, with differences typically ranging between 1.7% and 2.7%. A maximum difference of 4% at -0.5°C occurred between the real and simulated K^+-treated samples (Figure 2.8e). At temperatures below -5°C, unfrozen water contents for the real Copper River and simulated soils remain within 1% of each other. Differences in the unfrozen

water contents of the real and simulated soils may be attributed to the heterogeneous nature of the actual Copper River sample and errors in the semi-quantitative XRD analysis.

2.6 Conclusion

We determined the unfrozen water content of a suite of frozen, cation-treated, fine-grained soils using a P-NMR device and the normalization method, which demonstrated excellent repeatability and accuracy for separately prepared and tested samples. The overall set of tested samples included five standard clays that are commonly found in soils, and one heterogeneous soil, representing a comprehensive data set. Results indicated that cation treatments have negligible effect on the unfrozen water content of kaolinite, and minimal effect on illite, chlorite, and the heterogeneous soil (Copper River). Conversely, soils that are partially or completely composed of smectite demonstrated the largest unfrozen water content when treated with Na^+ cations. These same soils demonstrated a marked reduction in unfrozen water content with the K^+ treatment. Using the results from the standard clays, we estimated the unfrozen water content for a natural heterogeneous soil. Differences between the estimated and measured unfrozen water content ranged between 1% and 4% for all of the cation treatments, indicating that the unfrozen water content of a heterogeneous soil with a known mineralogy may be approximated from a database of measured unfrozen water contents for standard clays. Based on these positive results, this approach can be used to approximate changes in unfrozen water content in an *in situ* soil due to natural cation infiltration or leaching.

Future research with these soils will include measurement of their zeta potentials and soil micro-fabric, as well as the mobility of the unfrozen water within the frozen soil. As the results presented here use the new normalization method with the P-NMR device, we recommend comparing these results to those obtained for the same soils using other methods, such as TDR or DSC.

2.7 Acknowledgements

The authors thank R. Sinnok and Y. Miao for their time spent preparing the cation-treated samples, and Y. Miao for his many hours spent working on the temperature stability of the P-NMR system. This research was supported by the National Science Foundation (NSF) under Grant Number 1147806.

2.8 Disclaimer

The views, opinions, findings, and conclusions reflected in this paper are the responsibility of the authors only and do not represent the official policy or position of the NSF, or other entity.

2.9 Figures

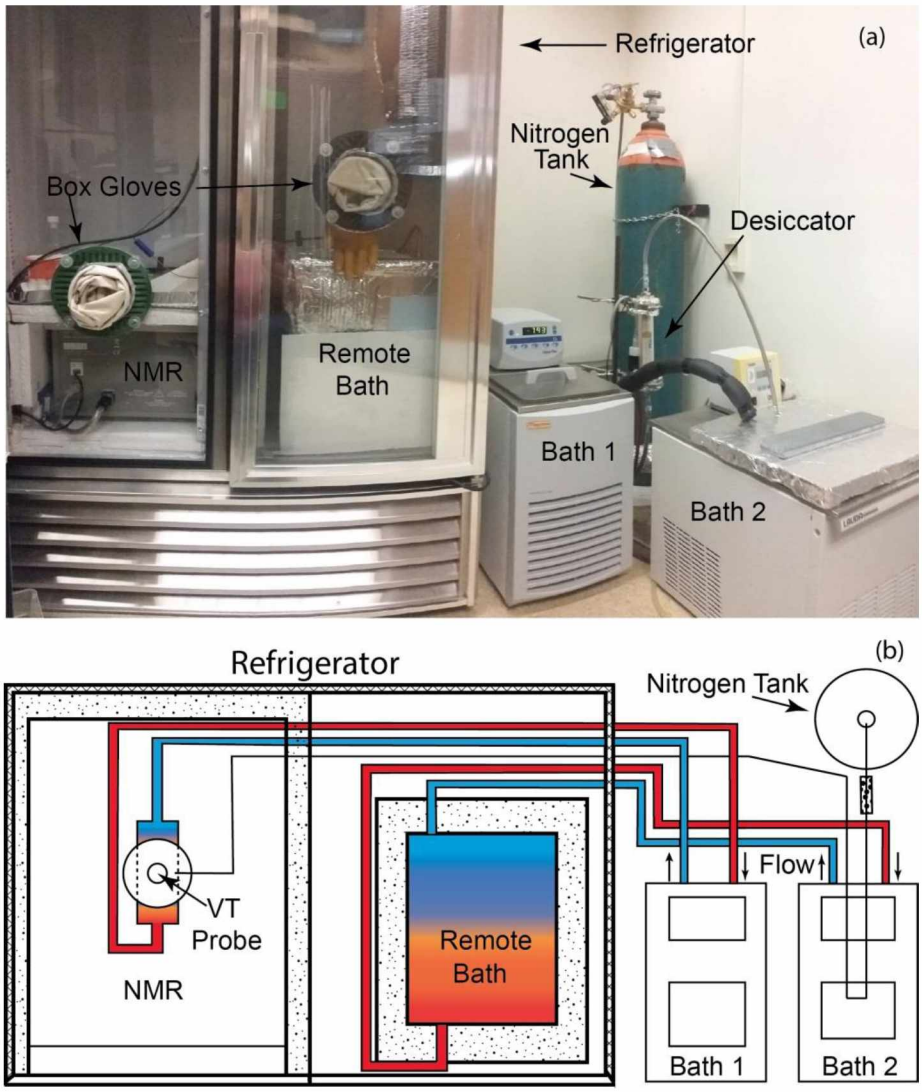

Figure 2.1 Laboratory equipment used for unfrozen water content measurement: (a) annotated photograph of equipment; (b) plan view schematic illustrating fluid flow from refrigerated circulating baths and nitrogen gas.

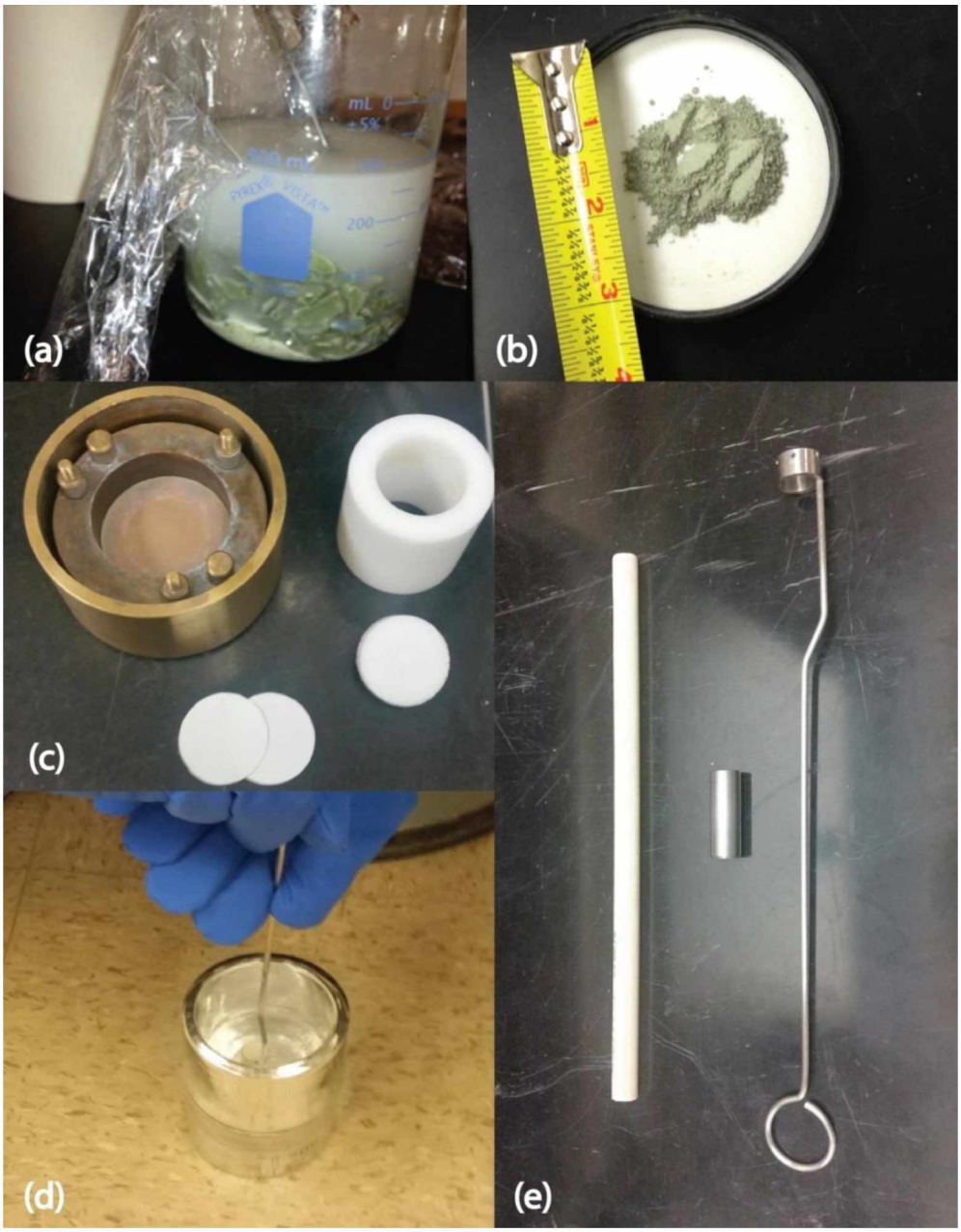

Figure 2.2 Images of sample preparation: (a) rock chips of Ripidolite (chlorite) (photograph courtesy of Y. Miao); (b) prepared chlorite powder (photograph courtesy of Y. Miao); (c) modified consolidation cell with plunger (white ring and plug) placed inside original loading cell with filter paper placed at top and bottom of soil slurry; (d) sample is flash frozen inside Dewar containing liquid nitrogen; (e) dowel, coring tool, and machined ladle for dipping coring tool with sample into liquid nitrogen.

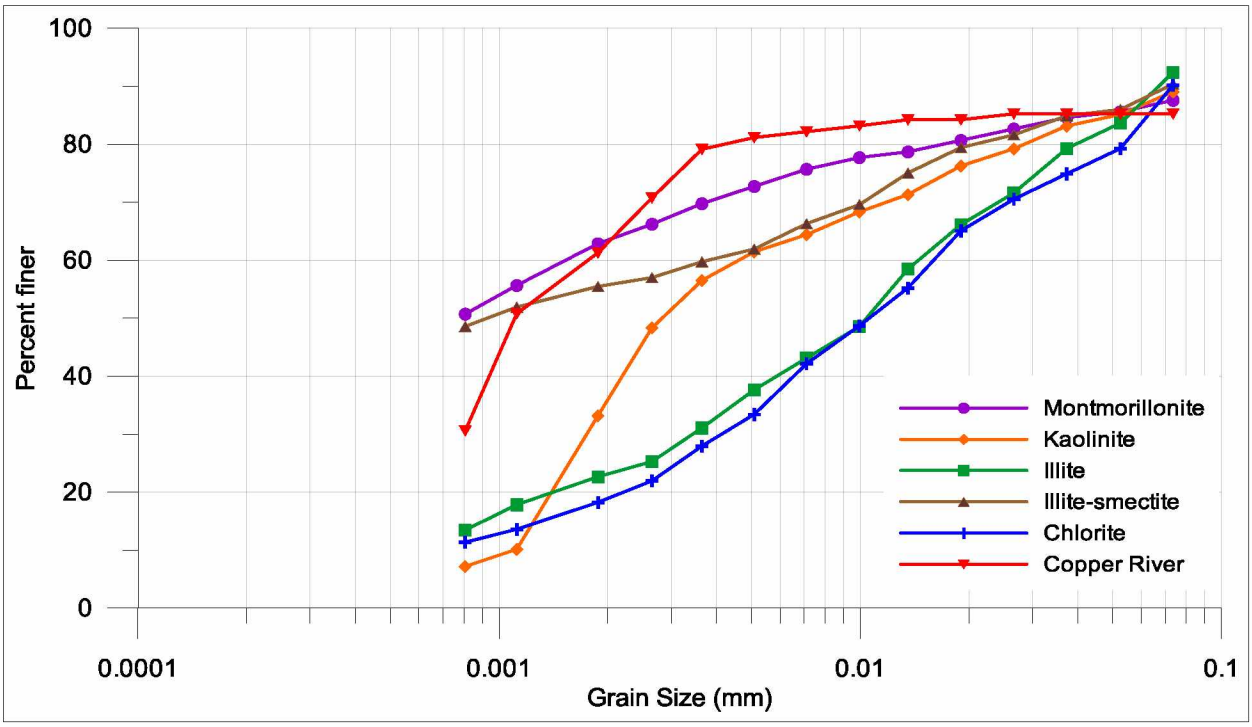

Figure 2.3 Sieve analysis for montmorillonite, kaolinite, illite, illite-smectite, chlorite, and Copper River.

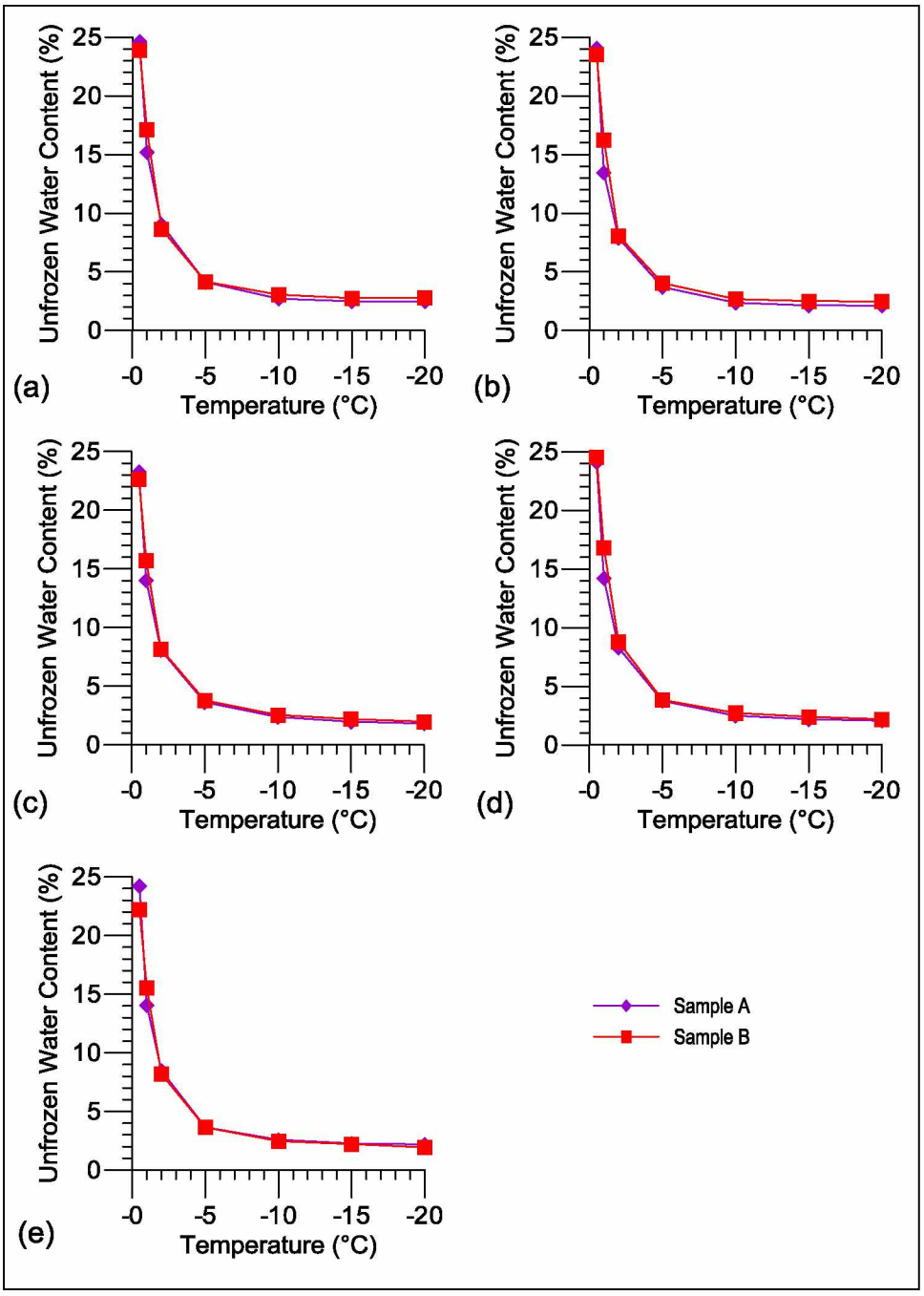

Figure 2.4 Comparison of unfrozen water content distribution curves for kaolinite samples A and B from two independent tests for experiment validation: (a) untreated; (b) Ca^{2+}; (c) Mg^{2+}; (d) Na^{+}; (e) K^{+}.

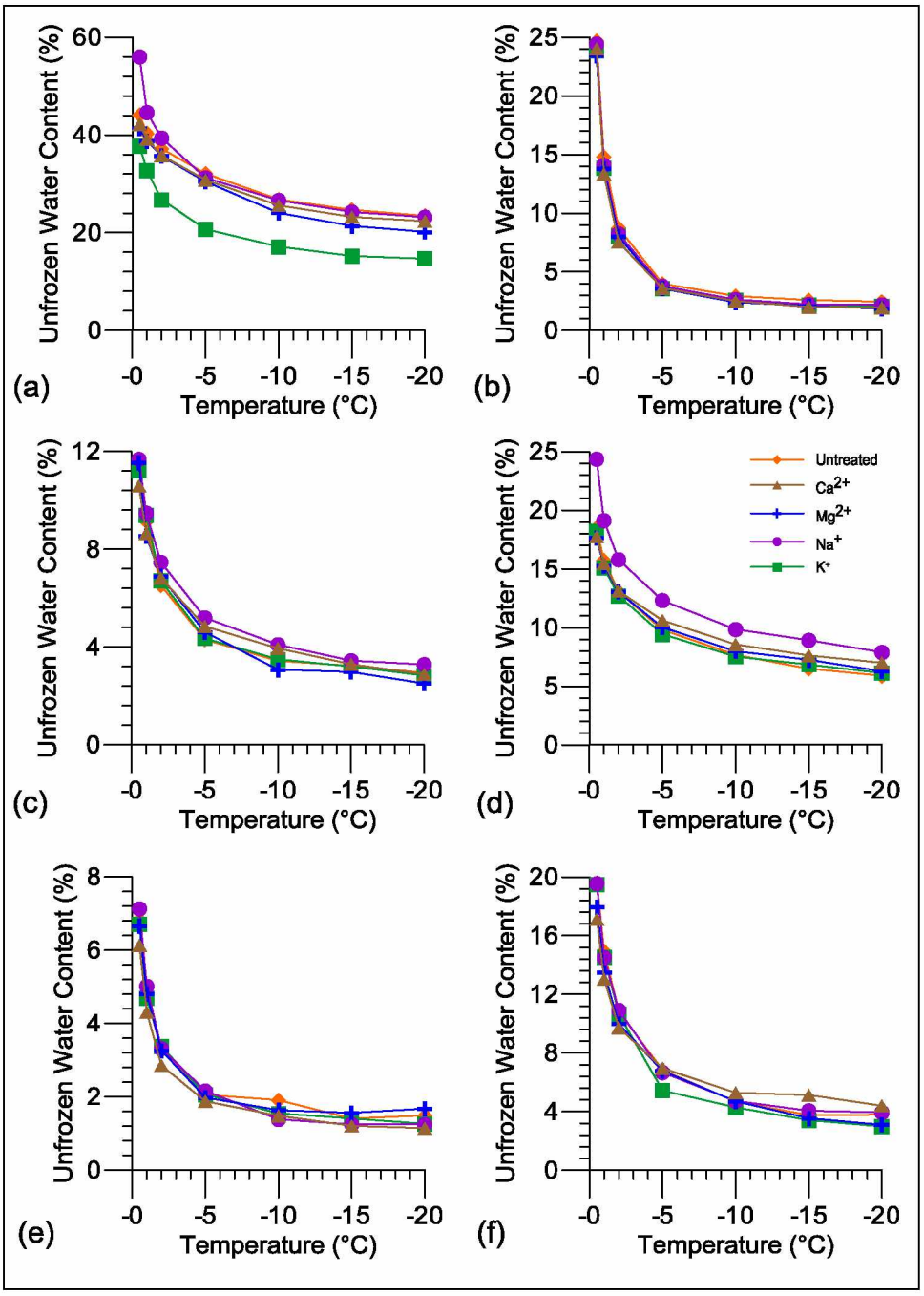

Figure 2.5 Comparison of unfrozen water content by clay: (a) montmorillonite; (b) kaolinite; (c) illite, (d) illite-smectite; (e) chlorite; (f) Copper River. Each sub-figure contains the results for the untreated and four cation-treated samples.

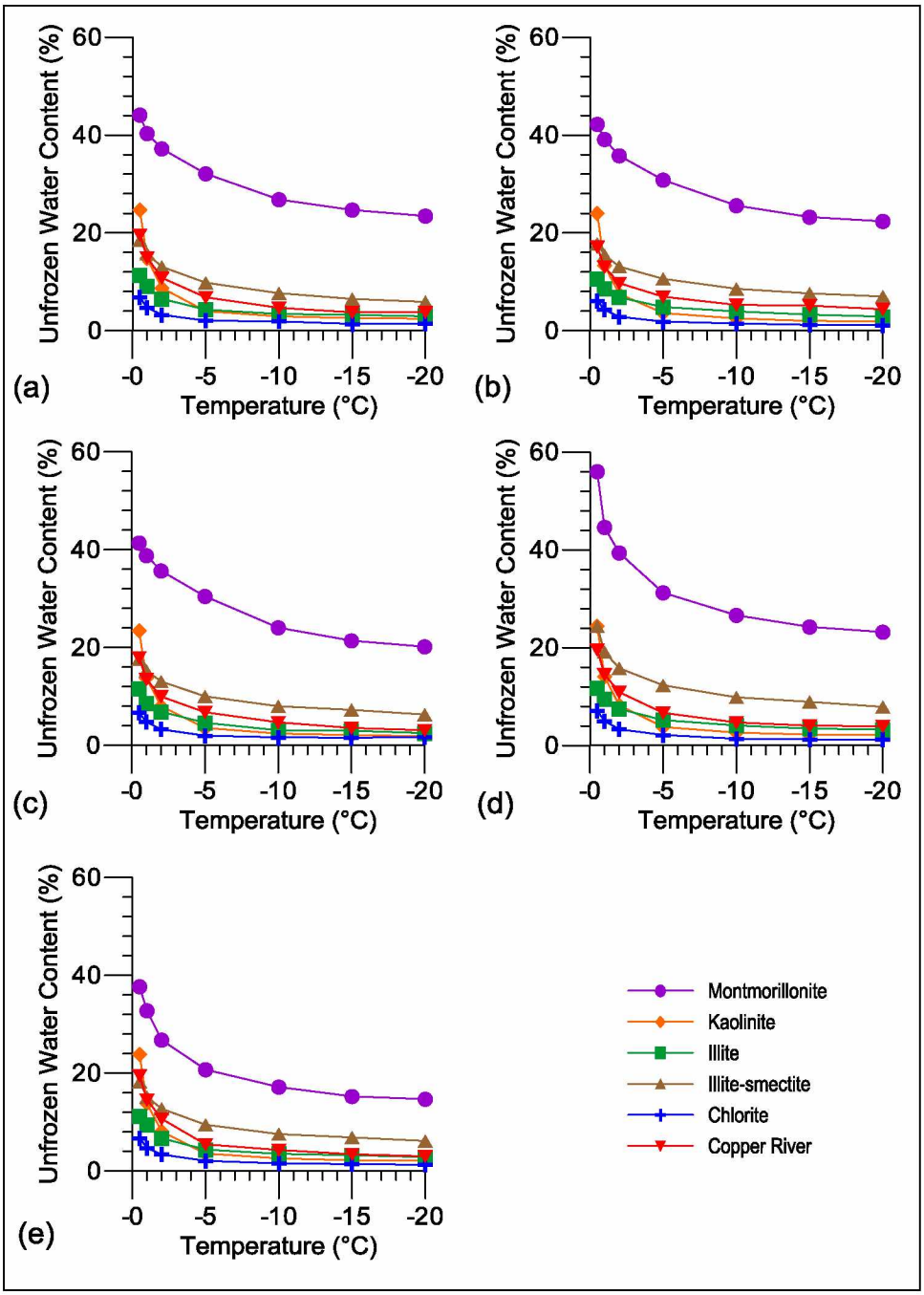

Figure 2.6 Comparison of unfrozen water content by cation treatment: (a) untreated, (b) Ca^{2+}; (c) Mg^{2+}; (d) Na^{+}; (e) K^{+}.

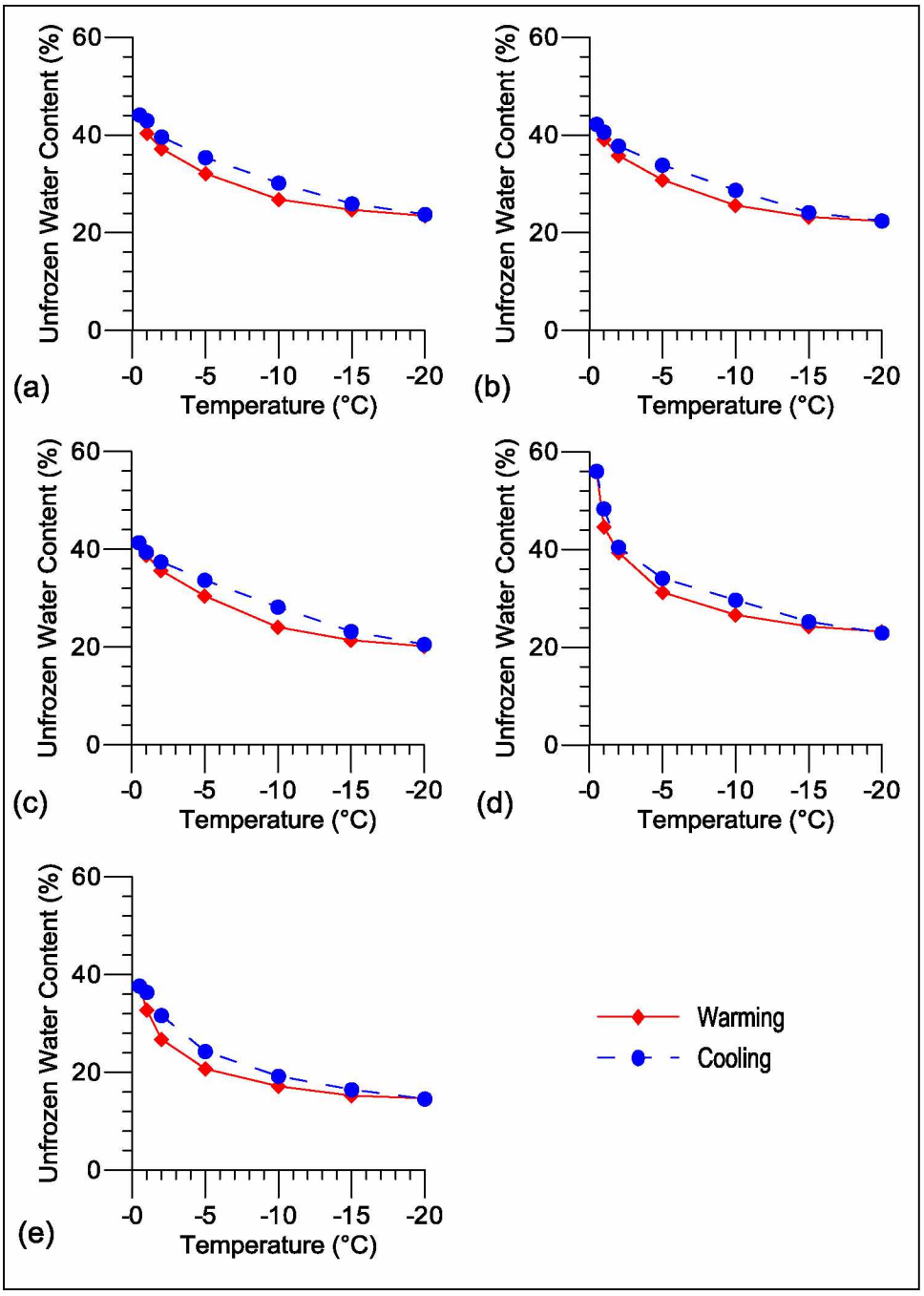

Figure 2.7 Hysteresis between the warming and cooling trends of the montmorillonite sample suite: (a) untreated; (b) Ca^{2+}; (c) Mg^{2+}; (d) Na^{+}; (e) K^{+}.

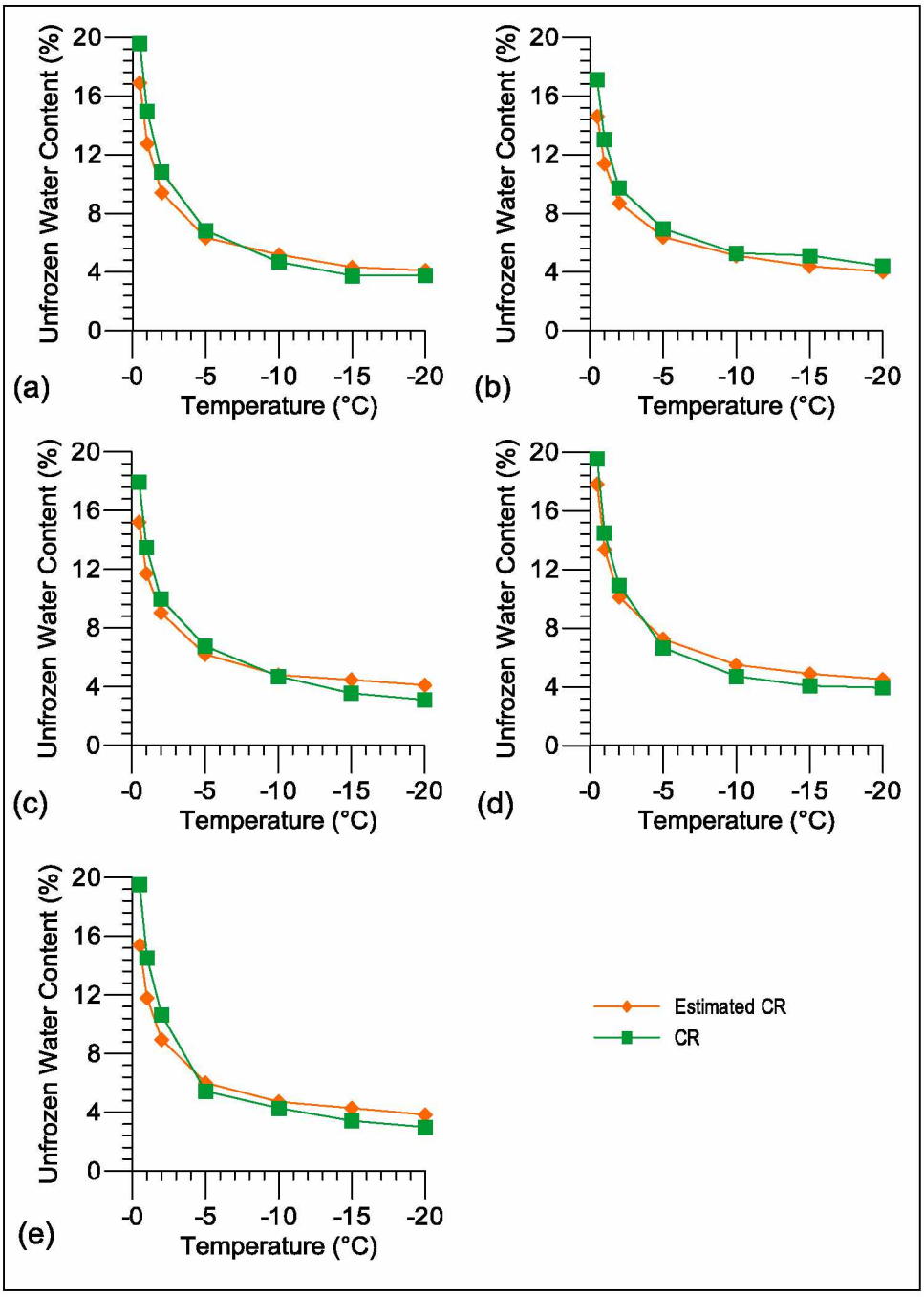

Figure 2.8 Comparison of actual Copper River (CR) unfrozen water content to that of a simulated soil (Estimated CR) using XRD data and results of tested source clays: (a) untreated; (b) Ca^{2+}; (c) Mg^{2+}; (d) Na^{+}; (e) K^{+}.

2.10 Tables

Table 2.1 Properties and origins of tested soils. Values with superscripts were taken from [1]Olphen and Fripiat (1979), [2]Jaynes and Bigham (1986), [3]Miller et al. (2012), [4]Geramian et al. (2016).

Soil (symbol)	Specific Gravity	Cation Exchange Capacity (cmol/kg)	Specific Surface Area (m^2/g)	Origin
Montmorillonite (STx-1b)	2.71	84.4[1]	83.8[1]	County of Gonzales, Texas
Kaolinite (KGa-2)	2.72	3.3[1]	23.5[1]	County of Warren, Georgia
Illite (IMt-1)	2.72	14.7[2]	31.5[3]	Silver Hill, Montana
Illite-smectite (ISCz-1)	2.72	37.5[4]	50.4[4]	Czech Republic
Chlorite (Cca-2)	2.73	1.0[2]	8.0[3]	Flagstaff Hill, California
Copper River (CR)	2.73	28.7	16.0	Copper River Basin, Alaska

Table 2.2 Copper River soil mineral composition based on XRD analysis. Values with superscripts are as follows: [1]Randomly Ordered Mixed-Layer Illite-Smectite, [2]Randomly Ordered Mixed-Layer Chlorite-Smectite, [3]Ordered Mixed-Layer Illite-Smectite, [4]Percent Smectite in Mixed-Layer Illite-Smectite. Rounding errors are present due to conversion from weight fraction to weight percent (K/T GeoServices, Inc., pers. comm., 2006).

Whole rock mineralogy	Weight %	Phyllosilicate mineralogy	Relative abundance (%)
Quartz	19.0	RO M-L I-S[1]	0
K-Feldspar	1.2	RO M-L C-S[2]	30
Plagioclase	47.0	O M-L I-S[3]	0
Amphibole	5.9	Illite & Mica	24
Calcite	0.8	Kaolinite	5
Pyrite	2.3	Chlorite	41
Total Phyllosilicates	24.0		
Total	100	Total	100
		%S in M-L I-S[4]	50

Table 2.3 Calculated dry densities and water contents after P-NMR testing. Values for the kaolinite suite are for repeatability tests Samples A and B, respectively.

Soil	Cation treatment	Gravimetric water content (%)	Dry density, p_d (g cm^{-3})	Volumetric water content (%)
Montmorillonite	Untreated	89.62	0.73	65.34
	Ca^{2+}	87.81	0.75	65.53
	Mg^{2+}	81.62	0.78	63.32
	Na^{+}	324.11	0.26	83.02
	K^{+}	136.49	0.53	72.41
Kaolinite	Untreated	57.76; 56.64	1.00; 0.96	57.61; 54.72
	Ca^{2+}	61.20; 60.27	0.94; 0.95	57.68; 57.15
	Mg^{2+}	54.28; 55.32	0.98; 1.00	53.36; 55.66
	Na^{+}	61.17; 60.04	0.94; 0.95	57.40; 56.94
	K^{+}	59.55; 58.38	0.96; 0.94	57.45; 54.86
Illite	Untreated	27.45	1.52	41.73
	Ca^{2+}	29.62	1.47	43.51
	Mg^{2+}	29.21	1.46	42.67
	Na^{+}	29.53	1.49	43.97
	K^{+}	30.32	1.46	44.16
Illite-smectite	Untreated	62.91	0.95	59.64
	Ca^{2+}	51.65	1.07	55.15
	Mg^{2+}	52.96	1.04	55.21
	Na^{+}	121.00	0.59	71.30
	K^{+}	96.10	0.72	69.03
Chlorite	Untreated	33.93	1.33	45.16
	Ca^{2+}	34.03	1.31	44.72
	Mg^{2+}	34.17	1.32	45.07
	Na^{+}	27.26	1.50	40.88
	K^{+}	34.76	1.33	46.28
Copper River	Untreated	55.20	1.04	57.34
	Ca^{2+}	57.27	1.02	58.39
	Mg^{2+}	55.48	1.05	58.22
	Na^{+}	64.42	0.96	61.96
	K^{+}	52.86	1.06	55.85

Table 2.4 Unfrozen water contents measured using the normalization method for all tested samples.

Soil	Cation treatment	Unfrozen water content (%) by temperature (°C)						
		-0.5	-1	-2	-5	-10	-15	-20
Montmorillonite	Untreated	44.11	40.32	37.19	32.10	26.83	24.69	23.46
	Ca^{2+}	42.21	39.12	35.79	30.82	25.59	23.24	22.37
	Mg^{2+}	41.39	38.79	35.68	30.46	24.06	21.39	20.16
	Na^{+}	56.00	11.61	39.39	21.24	26.63	24.25	23.19
	K^{+}	37.68	32.77	26.78	20.72	17.16	15.24	14.67
Kaolinite	Untreated	24.69	14.81	8.75	3.99	2.93	2.59	2.46
	Ca^{2+}	24.01	13.34	7.53	3.62	2.51	2.00	1.95
	Mg^{2+}	23.45	13.78	8.01	3.56	2.41	2.10	1.86
	Na^{+}	24.43	14.09	8.26	3.78	2.64	2.23	2.20
	K^{+}	23.84	13.82	8.07	3.56	2.57	2.17	2.10
Illite	Untreated	11.34	9.14	6.53	4.31	3.43	3.23	2.95
	Ca^{2+}	10.59	8.65	6.83	4.85	3.95	3.30	2.89
	Mg^{2+}	11.54	8.55	6.88	4.61	3.08	2.98	2.51
	Na^{+}	11.68	9.48	7.47	5.20	4.10	3.44	3.28
	K^{+}	11.23	9.40	6.71	4.35	3.50	3.20	2.83
Illite-smectite	Untreated	18.51	15.75	13.08	9.82	7.68	6.51	5.90
	Ca^{2+}	17.77	15.47	13.13	10.62	8.57	7.64	7.00
	Mg^{2+}	17.63	15.28	13.06	10.03	7.99	7.26	6.29
	Na^{+}	24.37	19.13	15.80	12.32	9.86	8.93	7.90
	K^{+}	18.24	15.11	12.72	9.44	7.53	6.86	6.13
Chlorite	Untreated	6.84	4.71	3.27	2.06	1.91	1.41	1.49
	Ca^{2+}	6.13	4.31	2.86	1.88	1.48	1.21	1.14
	Mg^{2+}	6.66	4.81	3.27	1.98	1.64	1.56	1.68
	Na^{+}	7.13	5.02	3.02	2.16	1.38	1.25	1.25
	K^{+}	6.71	4.68	3.38	2.06	1.55	1.41	1.26
Copper River	Untreated	19.60	14.95	10.83	6.83	4.68	3.76	3.79
	Ca^{2+}	17.12	13.03	9.73	6.96	5.29	5.13	4.40
	Mg^{2+}	17.96	13.51	9.98	6.77	4.70	3.55	3.10
	Na^{+}	19.56	14.52	10.92	6.67	4.72	4.06	3.95
	K^{+}	19.51	14.54	10.65	5.44	4.29	3.42	2.99

2.11 References

Akagawa, S., Iwahana, G., Watanabe, K., Chuvilin, E. M., Istomin, V. A. (2012). "Improvement of pulse NMR technology for determination of unfrozen water content in frozen soils." *Tenth International Conference on Permafrost, International Contributions:* The Northern Pub., Severnoye Izdatelstvo, Russia, 1, 21-25.

Aksenov, V. I., Klinova, G. I., Scheikin, I. V. (1998). "Material composition and strength characteristics of saline frozen soils." *Seventh International Conference on Permafrost,* Yellow Knife, Canada, *Collection Nordicana*, 55, 1-4.

Anderson, D. M., and Tice, A. R. (1973). "The unfrozen interfacial phase in frozen soil water systems." In *Ecological Studies: Analysis and Synthesis*, 4, 107-124.

ASTM. (1998). *D422 Standard Test Method for Particle-Size Analysis of Soils*: ASTM International, West Conshohocken, PA.

Atkins, P., and de Paula, J. (2002). *Physical Chemistry*, 7th Ed.: W. H. Freeman and Company, New York, NY.

Bouyoucos, G. W. (1917). *Classification and Measurement of the Different Forms of Water in the Soil by Means of the Dilatometer Method*: Technical Bulletin 36, Michigan Agricultural College Experiment Station, East Lansing, MI.

Bouyoucos, G. (1920). "A new classification of the soil moisture." *Soil Science,* 11(1), 33-47.

Cornell University. (1951). *Final Report, Soil Solidification Research, Cornell University 1946-1951: Vol. 2 - Fundamental Properties, Clay-Water Systems*: U.S. Department of Commerce, Washington, D. C.

Darrow, M. M., Huang, S. L., Akagawa, S. (2009). "Adsorbed cation effects on the frost susceptibility of natural soils." *Cold Regions Science and Technology*, 55, 263-277.

Darrow, M. M. (2011). "Thermal modeling of roadway embankments over permafrost." *Cold Regions Science and Technology*, 65, 474-487.

Fanning, D. S., and Keramidas, V. Z. (1977). "Micas." In Dixon, J. B. and Weed, S. B. (Eds.), *Minerals in Soil Environments*: Soil Science Society of America, Madison, WI., 195-258.

Geramian, M., Osacky, M., Ivey, D. G., Liu, Q., Etsell, H. (2016) "Effect of swelling clay minerals (montmorillonite and illite-smectite) on nonaqueous bitumen extraction from Alberta Oil Sands." *Energy and Fuels,* American Chemical Society, <pubs.acs.org/doi/pdf/10.1021/acs.energyfuels.6b01026>, (Oct. 16, 2016).

Grim, R. E. (1952) "Relation of frost action to the clay-mineral composition of soil materials." *Highway Research Board, Proc., Annual Meeting*, 2, 167-172.

Grim, R. E. (1958). "Organization of water on clay mineral surfaces and its implication for the properties of clay-water systems." *National Research Council, Highway Research Board*, 40, 17-23.

Heagler, J. B. (1964). "Clay mineralogy and soil stabilization." *Proceedings of the Fifteenth Annual Highway Geology Symposium*, Rolla, Miss., 133-138.

Hillel, D. (1998). *Environmental Soil Physics*: Academic Press, San Diego, CA., 159-161.

Hoekstra, P. (1966). "Moisture movement in soils under temperature gradients with the cold-side temperature below freezing." *Water Resources Research,* 2(2), 241-250.

Ishizaki, T., Maruyama, M., Furukawa, Y., Dash, J. G. (1996). "Premelting of ice in porous silica glass." *Journal of Crystal Growth*, 163, 455-460.

Jaynes, W. F., and Bigham, J. M. (1986). "Multiple cation-exchange capacity measurements on standard clays using a commercial mechanical extractor." *Clays and Clay Minerals,* 34(1), 93-98.

Kiselev, V. F., Kvlividze, V. I., Kurzayev, A. B. (1973). "Surface phenomena at the ice-gas and ice-solid interfaces." *Proc., Permafrost; Second International Conference, USSR Contribution*, National Research Council of Canada, National Academy of Science, Yakutsk, U.S.S.R., 339-341.

Klein, J., and Jessberger, H. L. (1976). "Creep stress analysis of frozen soils under multiaxial states of stress." *Engineering Geology*, 13, 353-365.

Konrad, J. M., and Morgenstern, N. R. (1983). "Frost susceptibility of soils in terms of their segregation potential." *Proc., Permafrost: Fourth International Conference*, University of Alaska Fairbanks and National Academy of Sciences, Fairbanks, AK, 660-665.

Kozlowski, T. (2003). "A comprehensive method of determining the soil unfrozen water curves, 2. Stages of the phase change process in frozen soil-water system." *Cold Regions Science and Technology*, 36, 81-92.

Kruse, A. M., Darrow, M. M., Akagawa, S. (In review). "Improvements in measuring unfrozen water in frozen soils using the pulse nuclear magnetic resonance (P-NMR) method." *Journal of Cold Regions Engineering.*

Lambe, W. (1953). "The structure of inorganic soil." *Proc., ASCE*, 79(315), 1-49.

Lambe, T. W., Kaplar, C. W., Lambie, T. J. (1969). *Effect of Mineralogical Composition of Fines on Frost Susceptibility of Soils*: CRREL Report TR-207, US Army Cold Regions Research and Engineering Laboratory, Hanover, NH.

Macht, F., Eusterhues, K., Pronk, G. J., Totsche, K. U. (2011). "Specific surface area of clay minerals: Comparision between atomic force microscopy measurements and bulk-gas (N_2) and liquid (EGME) adsorption methods." *Applied Clay Science,* 53, 20-26.

Martin, R. T. (1960). *Adsorbed Water on Clay: A Review*: Massachusetts Institute of Technology, MA, 42 p.

McBride, M. B. (1994). *Environmental Chemistry of Soils:* Oxford University Press, Inc., New York, NY.

Miller, A., Kruichiak, J., Tellez, H., Wang, Y. (2012). "Iodide sorption to clays and the relationship to surface charge and clay texture." *Proc., Annual Radioactive Waste Management Conference*, Phoenix, AZ, 1-12.

Miller, R. D. (1978). "Frost heaving in non-colloidal soils." *Proc., Third International Conference on Permafrost*, National Research Council of Canada, Edmonton, Alberta, Canada, 707-713.

Nersesova, F. A. and Tsytovich, V. A. (1963). "Unfrozen water in frozen soils." *Proc., Permafrost; First International Conference*, *Lafayette, IN,* National Academy of Science, National Research Council, Washington, D.C., 230-234

Odom, I. E. (1984). "Smectite clay minerals: properties and uses." *Philosophical Transactions of the Royal Society, London*, A311, 391-409.

Olphen, H. V., and Fripiat, J. J. (Eds). (1979). *Data Handbook for Clay Materials and Other Non-metallic Minerals:* Pergamon Press, Inc., New York, NY.

Oxford Instruments. (2006). *MARAN Ultra Non-Expert User Manual*: Oxford Instruments Ltd., Tubney Wood, Abingdon, UK.

Patterson, D. E., and Smith, M. W. (1980). *The Measurement of Unfrozen Water Content by Time Domain Reflectometry: Results from Laboratory Tests:* Carleton University, Ottawa, Ontario.

Romanovsky, V. E., and Osterkamp, T. E. (2000). "Effects of unfrozen water on heat and mass transport processes in the active layer and permafrost." *Permafrost and Periglacial Processes*, 11, 219-239.

Smith, M. W., and Tice, A. R. (1988). *Measurement of the Unfrozen Water Content of Soils*: CRREL Report 88-18, US Army Cold Regions Research and Engineering, Hanover, NH.

Tan, K. (1998). *Principles of Soil Chemistry, 3rd Ed:* Marcel Dekker, Inc., New York, NY.

Taylor, S. A. and Ashcroft, G. L. (1972). *Physical Edaphology – The Physics of Irrigated and Nonirrigated Soils*: W. H. Freeman and Company, San Francisco, CA.

Theng, B. K. G. (1972). "Formation, properties, and practical applications of clay-organic complexes." *Journal of the Royal Society of New Zealand,* 2(4), 437-457.

Tian, H., Wei, C., Wei, H., Zhou, J. (2014). "Freezing and thawing characteristics of frozen soils: bound water content and hysteresis phenomenon." *Cold Regions Science and Technology*, 103, 74-81.

Tice, A. R., and Oliphant, J. L. (1984). "The effect of magnetic particles on the unfrozen water content of frozen soils determined by nuclear magnetic resonance." *Soil Science*, 138(1), 63-73.

Tice, A. R., Burrous, C. M., Anderson, D. M. (1978). "Determination of unfrozen water in frozen soil by pulsed nuclear magnetic resonance." *Third International Conference on Permafrost*, The National Research Council of Canada, Alberta, Canada, 1, 150-155.

Torrance, J. K., and Schellekens, F. J. (2006). "Chemical factors in soil freezing and frost heave." *Polar Record*, 42, 33-42.

Watanabe, K., and Wake, T. (2009). "Measurement of unfrozen water content and relative permittivity of frozen unsaturated soil using NMR and TDR." *Cold Regions Science and Technology*, 59, 34-41.

Williams, P. J. (1964). "Unfrozen water content of frozen soils and soil moisture suction." *Geotechnique*, 16(3), 187-208.

General Conclusions

Unfrozen water within frozen soils has been the focus of laboratory testing for over one hundred years. Although a variety of testing methods exist, the P-NMR method has been considered as a reliable standard for measuring unfrozen water content. Traditionally, unfrozen water content was measured using the first return values of the free-induction decay signal intensity. Results from this current research that indicate the traditional method may overestimate the unfrozen water content.

This study used a P-NMR testing facility and the normalization method to measure unfrozen water content. The P-NMR testing facility included modifications that maintained excellent temperature control of the P-NMR device and the tested samples, thereby eliminating many of the problems that previous authors experienced, such as detuning of the P-NMR magnet, or thermal variations within the samples due to the lack of a variable temperature (VT) probe. Results demonstrated that the testing methodology is both repeatable and accurate, based on a comparison of measurements from two independent testing facilities and a comparison of P-NMR measurements to physical gravimetric water content results derived from a desorption test. The results also indicated that the unfrozen water content in a frozen soil can dramatically vary for a given sub-freezing temperature depending on the time chosen after the 90° pulse for the calculations, significantly overestimating unfrozen water content. Using the normalization method removes the risk of inadvertently including ice content with the unfrozen water content.

The samples tested consisted of five standard clays commonly found in soil and one heterogeneous soil, each prepared into the untreated soil and four cation treatments. Results indicated that cations have varying impact on unfrozen water content dependent on the structure of the clay. Clays with large specific surface areas (SSA) and cation exchange capacities (CEC) yielded higher unfrozen water contents (especially for those treated with Na^{+})

over a greater sub-freezing temperature range, and lower unfrozen water contents for K^+ treatments. In contrast, clays with lower SSA and CEC (i.e., chlorite, illite, and kaolinite) demonstrated minimal to negligible responses of unfrozen water content to cation treatment.

The results of the five homogeneous clays were used to estimate the unfrozen water content of the heterogeneous Copper River sample. The estimated unfrozen water contents were within 4% of the measured unfrozen water contents for all cation treatments. This suggests that unfrozen water content may be estimated for a heterogeneous soil with a known mineralogy without testing physical samples, given a data base of unfrozen water content for standard clays.

As part of a larger research project, results from this P-NMR testing will be used in conjunction with measurements of zeta potential, micro-aggregates, and micro-fabric for this same set of soils to improve our understanding of the mass and mobility of unfrozen water in frozen soils, and thus the behavior of frozen ground. As the results presented in this thesis use the new normalization method with the P-NMR device, it is recommended to compare these results to those obtained using alternate methods, such as time-domain reflectometry (TDR) or differential scanning calorimetry (DSC).

References

Akagawa, S. (1988). "Experimental study of frozen fringe characteristics." *Cold Regions Science and Technology*, 15, 209-223.

Darrow, M. M. (2011). "Thermal modeling of roadway embankments over permafrost." *Cold Regions Science and Technology*, 65, 474-487.

Ferrians, O. J., Kachadoorian R., Greene, G. W., (1969). *Permafrost and Related Engineering Problems in Alaska*: U.S. Geological Survey Professional Paper 678, U.S. Dept. of the Interior, U.S. Government Printing Office, Washington, D.C.

Grim, R. E. (1952) "Relation of frost action to the clay-mineral composition of soil materials." *Highway Research Board, Proc., Annual Meeting*, 2, 167-172.

Johnston, B., Ladanyi, B., Morgenstern, N.R., Penner, E. (1981). "Engineering characteristics of frozen and thawing soils." In: *Permafrost Engineering Design and Construction*, Wiley & Sons, Toronto, Ontario, 73-147.

Krahn, J. (2004). *Thermal Modeling with TEMP/W: an Engineering Methodology.* GEO-SLOPE International, Ltd., Calgary, Alberta.

Lai, Y., Pei, W., Zhang, M., Zhou, J. (2014). "Study on theory model of hydro-thermal-mechanical interaction process in saturated freezing silty soil." *International Journal of Heat and Mass Transfer*, 78, 805-819.

Lambe, W. (1953). "The structure of inorganic soil." *Proc., ASCE*, 79(315), 1-49.

Lambe, T. W., Kaplar, C. W., Lambie, T. J. (1969). *Effect of Mineralogical Composition of Fines on Frost Susceptibility of Soils*: CRREL Report TR-207, US Army Cold Regions Research and Engineering Laboratory, Hanover, NH.

Marchenko, S., Romanovsky, V., Tipenko, G. (2008). "Numerical modeling of spatial permafrost dynamics in Alaska." *Proc., Permafrost: Ninth International Conference on Permafrost,* University of Alaska Fairbanks, Institute of Northern Engineering, Fairbanks, AK, 1125-1130.

Nersesova, F. A. and Tsytovich, V. A. (1963). "Unfrozen water in frozen soils." *Proc., Permafrost; First International Conference*, *Lafayette, IN,* National Academy of Science, National Research Council, Washington, D.C., 230-234

Patterson, D. E., and Smith, M. W. (1980). *The Measurement of Unfrozen Water Content by Time Domain Reflectometry: Results from Laboratory Tests*: Carleton University, Ottawa, Ontario.

Tice, A. R., Black, P. B., Berg, R. L. (1989). "Unfrozen water contents of undisturbed and remolded Alaskan Silt." *Cold Regions Science and Technology,* 17, 103-111.

Tice, A. R., Oliphant, J. L., Nakano, Y., Jenkins, T. F. (1982) *Relationship Between the Ice and Unfrozen Water Phases in Frozen Soil as Determined by Pulsed Nuclear Magnetic Resonance and Physical Desorption Data.* CRREL Report 82-15, US Army Cold Regions Research and Engineering Laboratory, Hanover, NH.

Torrance, J. K., and Schellekens, F. J. (2006). "Chemical factors in soil freezing and frost heave." *Polar Record*, 42, 33-42.

Zhang, L., Ma, W., Yang, C., Yuan, C. (2014). "Investigation of the pore water pressures of coarse-grained sandy soil during open-system step-freezing and thawing tests." *Engineering Geology*, 181, 233-248.

Zhou, J., Wei, C., Li, D., Wei, H. (2014). "A moving-pump model for water migration in unsaturated freezing soil." *Cold Regions Science and Technology*, 104-105, 14-22.

Appendices

Appendix A Cooling Trends for Cation-Treated Soils

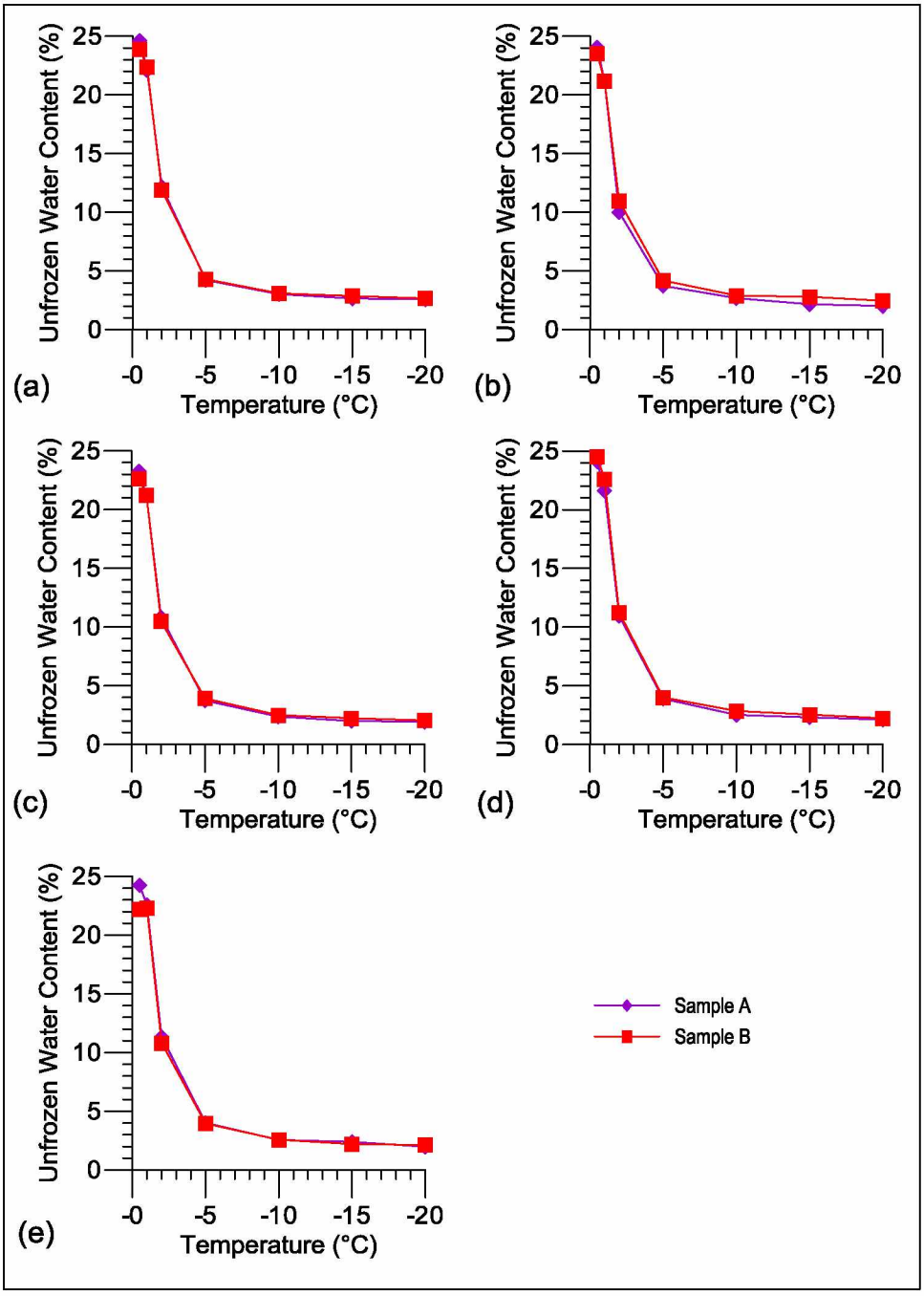

Figure A-1 Comparison of unfrozen water content distribution curves for kaolinite samples A and B from two independent tests for experiment validation: (a) untreated; (b) Ca^{2+}; (c) Mg^{2+}; (d) Na^{+}; (e) K^{+}.

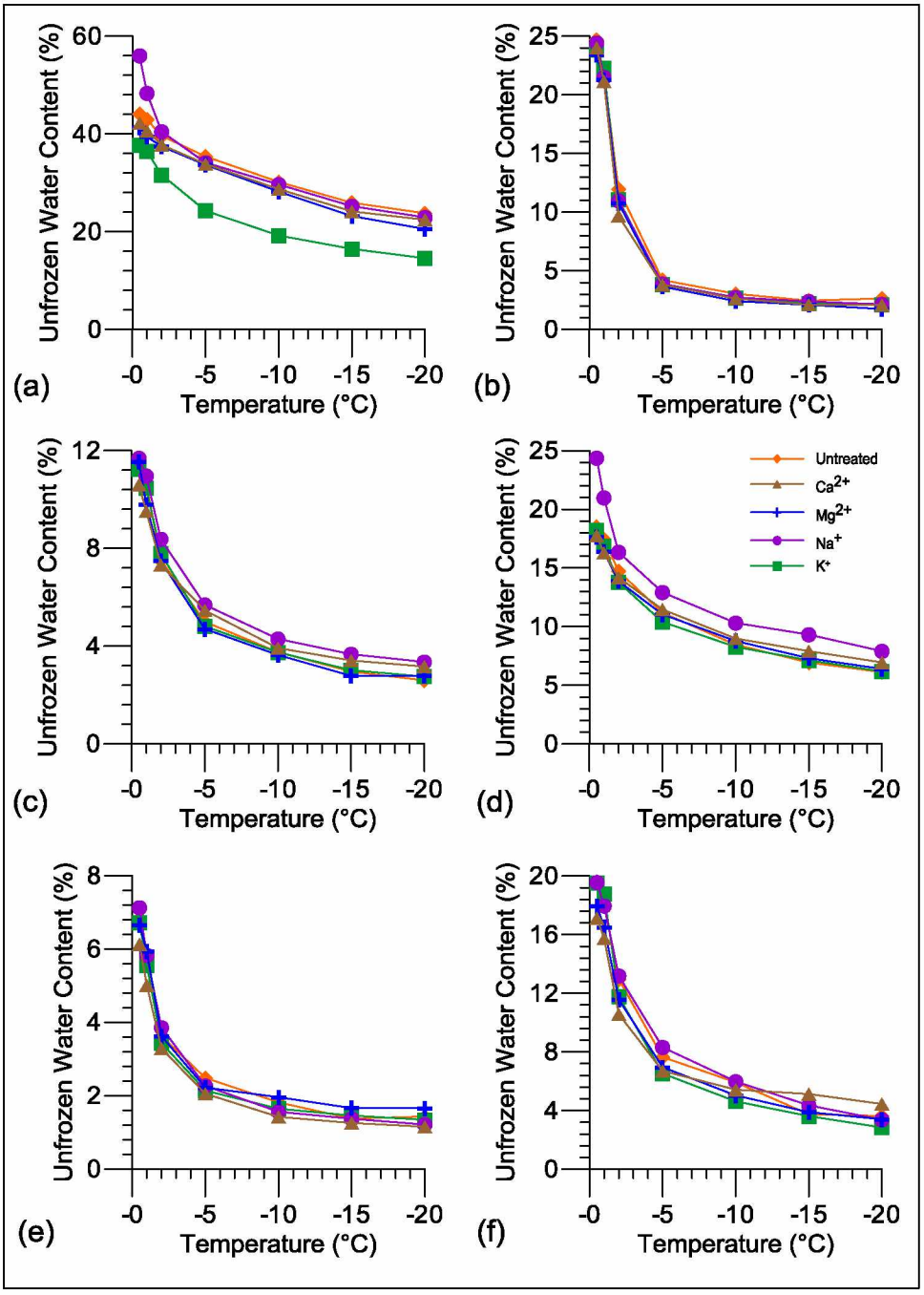

Figure A-2 Comparison of unfrozen water content by clay: (a) montmorillonite; (b) kaolinite; (c) illite, (d) illite-smectite; (e) chlorite; (f) Copper River. Each sub-figure contains the results for the untreated and four cation-treated samples.

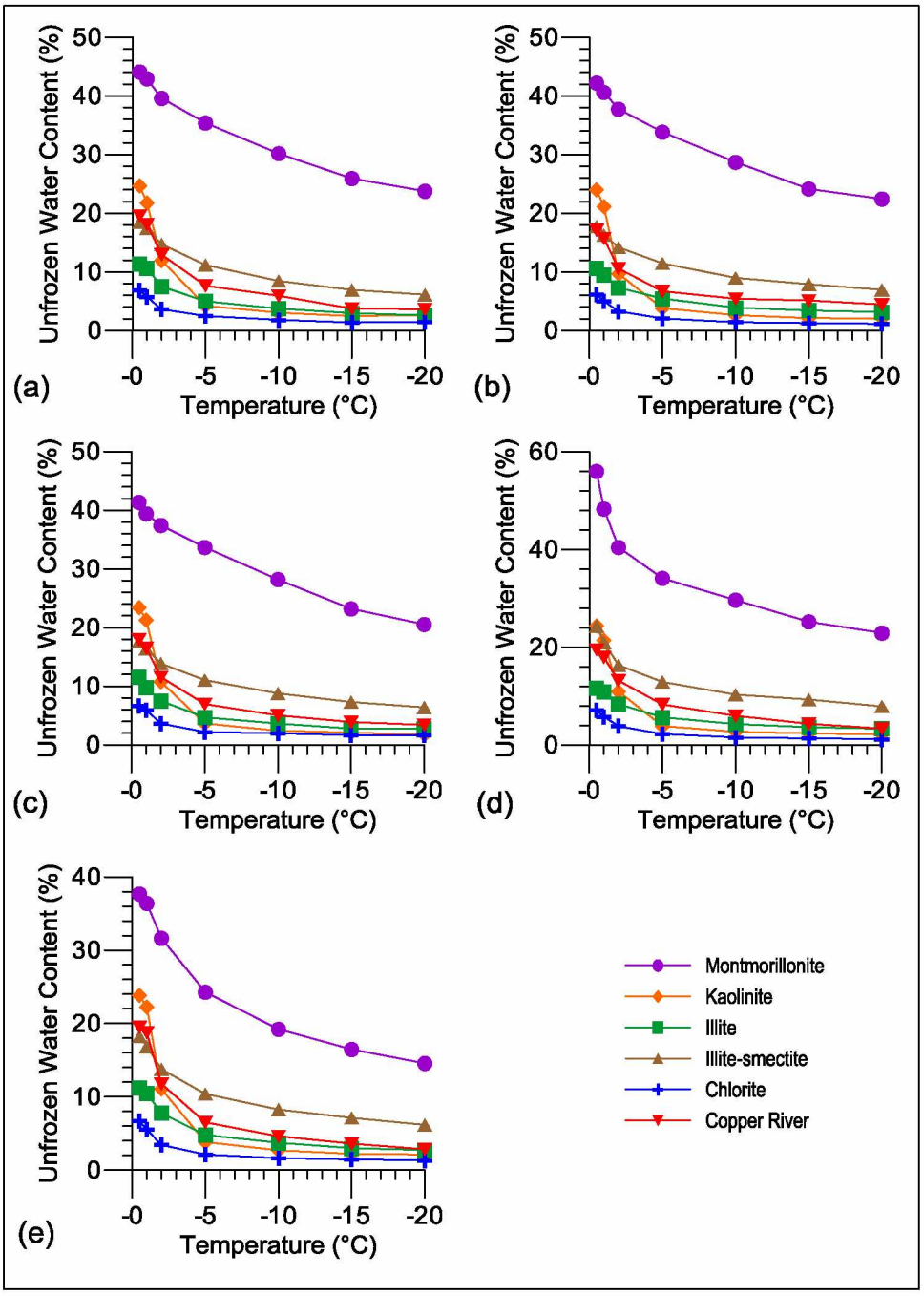

Figure A-3 Comparison of unfrozen water content by cation treatment: (a) untreated, (b) Ca^{2+}; (c) Mg^{2+}; (d) Na^{+}; (e) K^{+}.

Appendix B Hysteresis Effects of Cation-Treated Soils

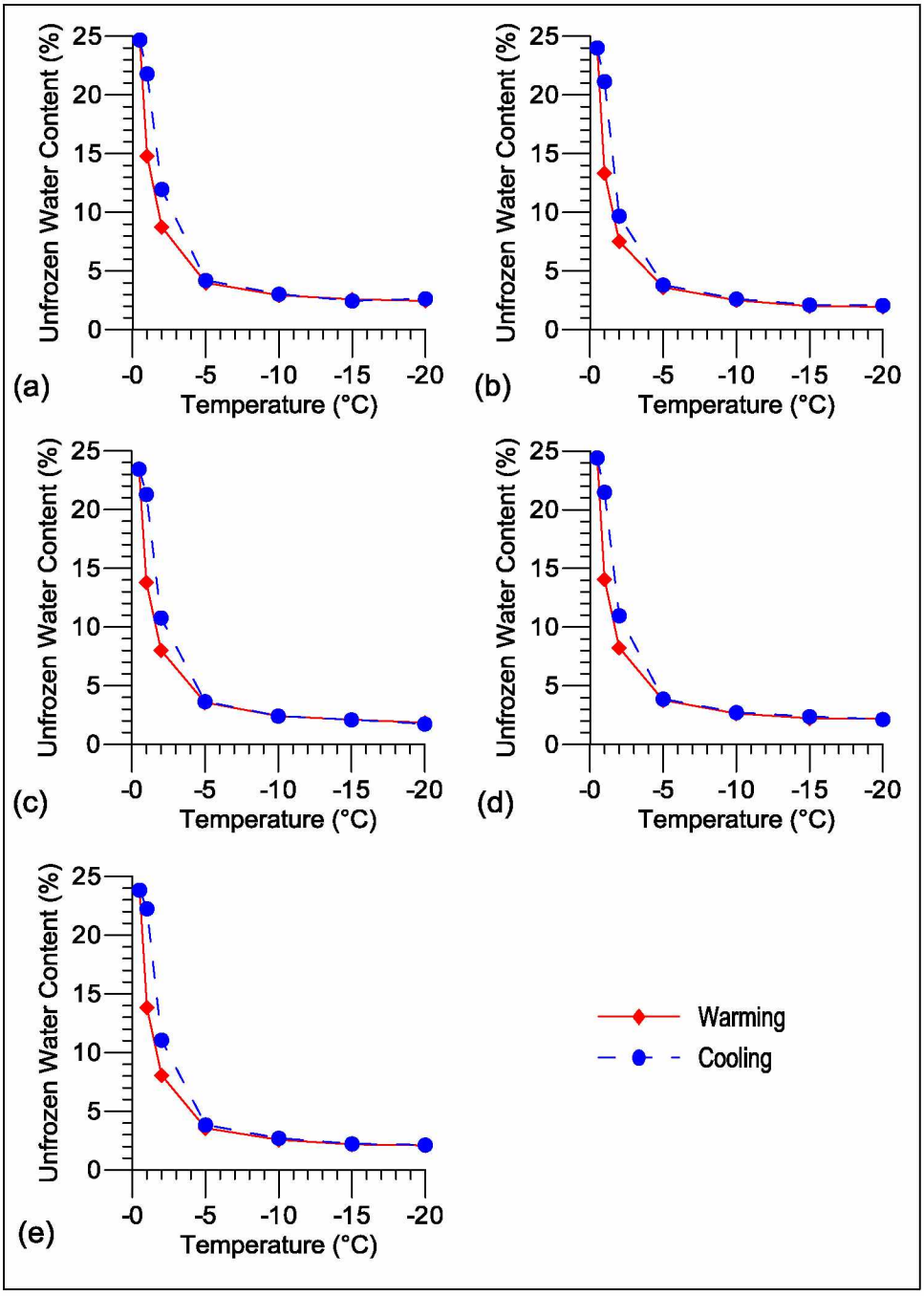

Figure B-1 Hysteresis effects of kaolinite: (a) untreated, (b) Ca^{2+}, (c) Mg^{2+}, (d) Na^{+}, (e) K^{+}.

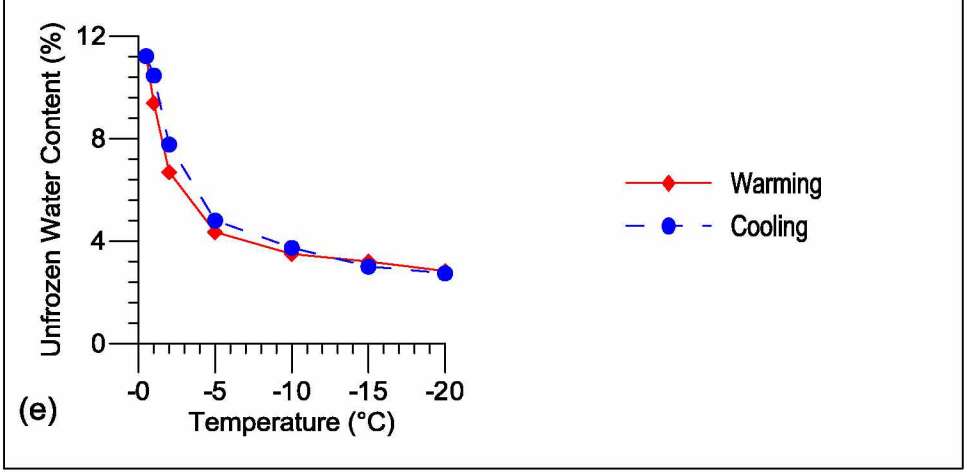

Figure B-2 Hysteresis effects of illite: (a) untreated, (b) Ca^{2+}, (c) Mg^{2+}, (d) Na^{+}, (e) K^{+}.

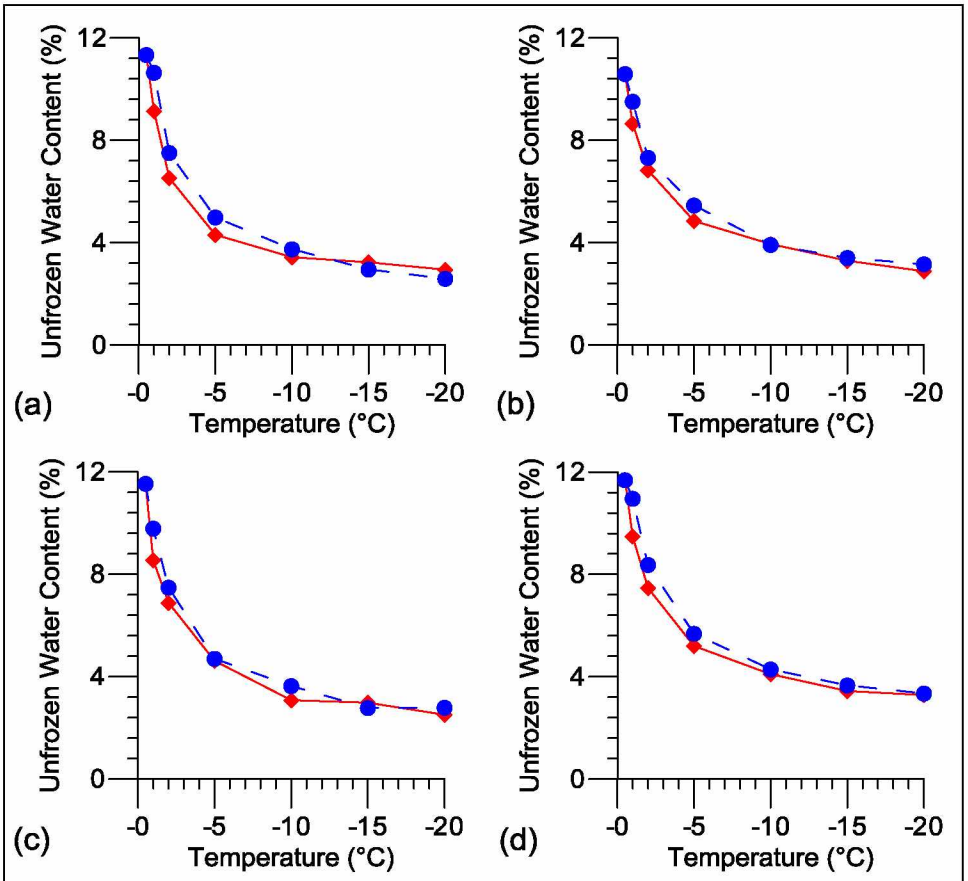
Unfrozen Water Content (%)
12
8
4
0
-0
-5
-10
-15
-20
Temperature (°C)
(a)
(b)
(c)
(d)

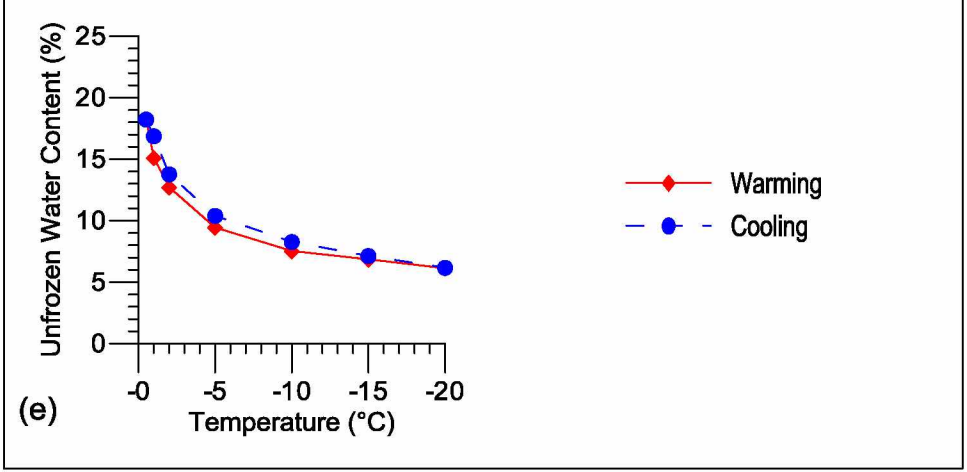

Figure B-3 Hysteresis effects of illite-smectite: (a) untreated, (b) Ca^{2+}, (c) Mg^{2+}, (d) Na^{+}, (e) K^{+}.

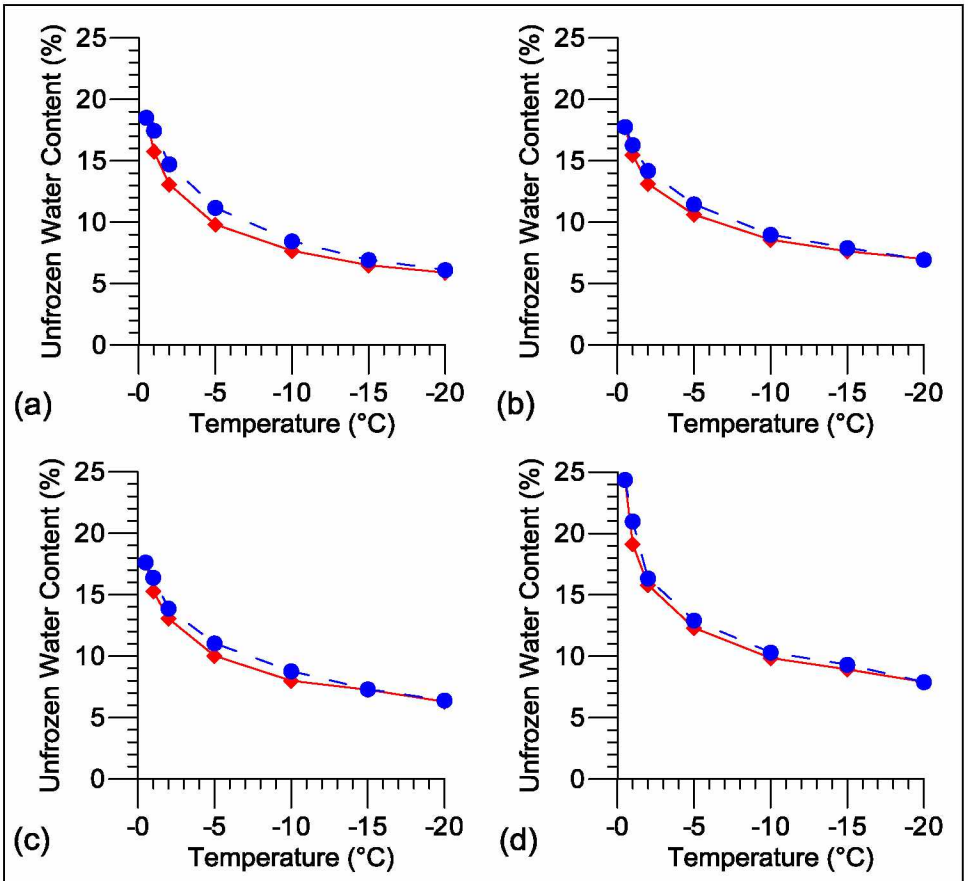
Unfrozen Water Content (%)
25
20
15
10
5
0
-0
-5
-10
-15
-20
Temperature (°C)
(a)
(b)
(c)
(d)

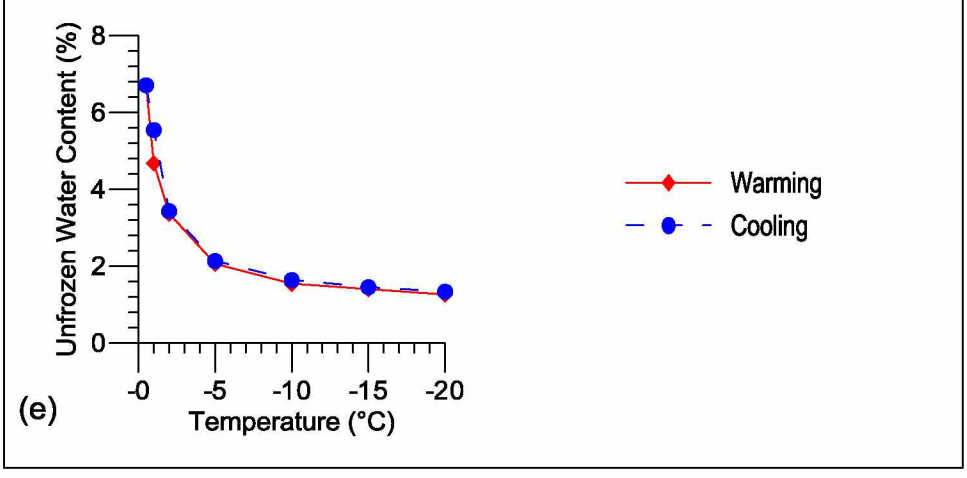

Figure B-4 Hysteresis effects of chlorite: (a) untreated, (b) Ca^{2+}, (c) Mg^{2+}, (d) Na^{+}, (e) K^{+}.

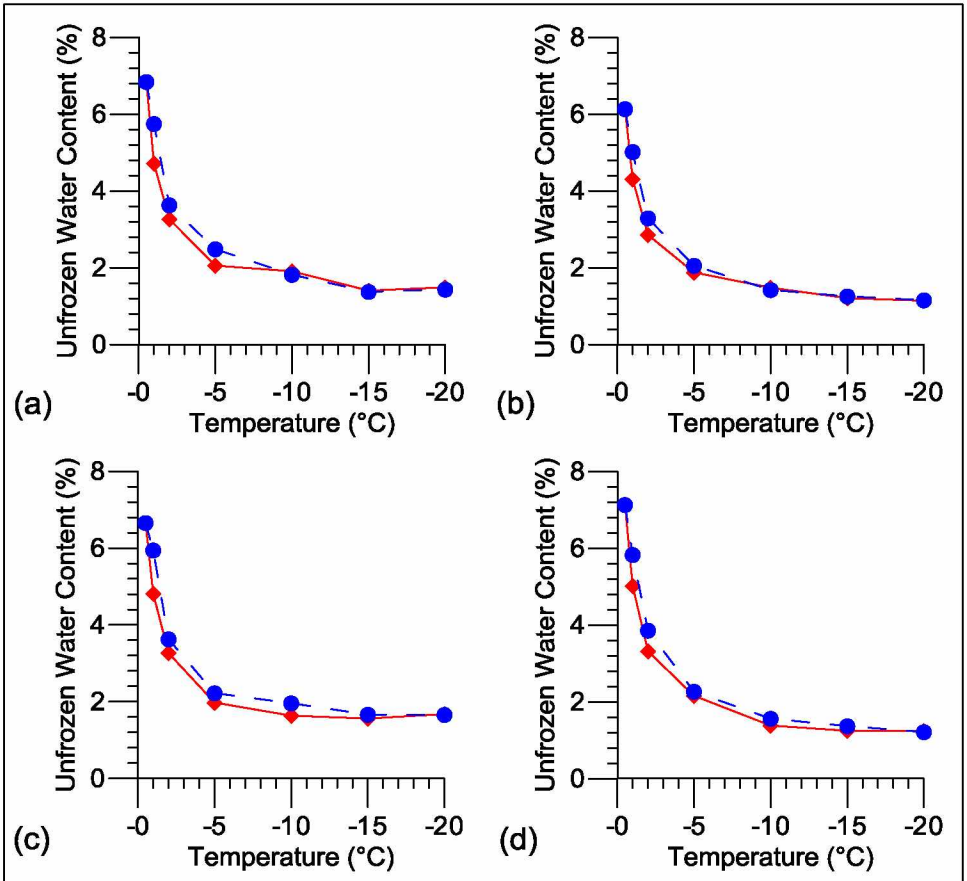
Unfrozen Water Content (%)
0
2
4
6
8
-0
-5
-10
-15
-20
Temperature (°C)
(a)
(b)
(c)
(d)

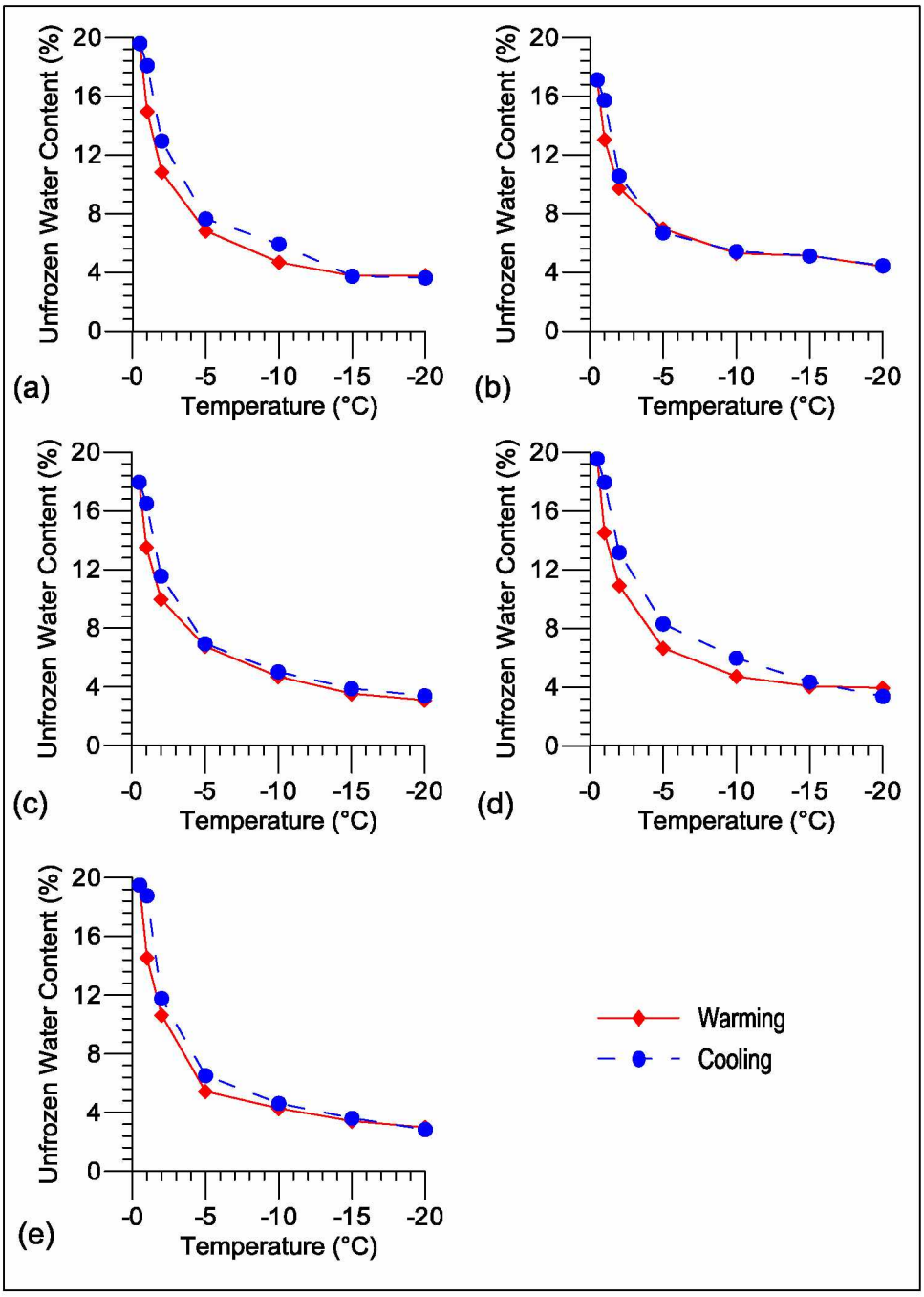

Figure B-5 Hysteresis effects of Copper River: (a) untreated, (b) Ca^{2+}, (c) Mg^{2+}, (d) Na^{+}, (e) K^{+}.